École polytechnique fédérale de Lausanne -
Københavns Universitet

Master Thesis

Copenhagen Centre for Geometry and Topology

Homology of Sullivan diagrams

Author:
Juan Felipe Celis Rojas

Supervisor:
Nathalie Wahl
EPFL Responsible:
Jérôme Scherer

Abstract

We study the homology of the harmonic compactification of the moduli space of Riemann surfaces. This compactification admits a combinatorial model using metric fat graphs, known as Sullivan diagrams. First, we present new computations of the fundamental groups of spaces of Sullivan diagrams. Next, we provide a new proof of homological stability for Sullivan diagrams with respect to the number of punctures and boundary components. As part of this proof, we compute the stable homology of the spaces of Sullivan diagrams.

Acknowledgments

I would like to thank Nathalie for receiving me this semester at Copenhagen. It has been a wonderful experience. I am grateful for all I learned with you at the GeoTop centre.

I also want to thank Jérôme Scherer for guiding me throughout my master and encouraging me to do my master thesis abroad.

Introduction

We study the homology of the harmonic compactification of the moduli space of Riemann surfaces. Two decades ago Bödigheimer [4] proved that this moduli space of Riemann surfaces admits a combinatorial model using graphs. An important feature of this model is its so-called *harmonic compactification*. While certain results about the moduli space translate directly to this compactification, much about its structure and properties remains to be understood.

In recent years, several papers have explored different constructions of the harmonic compactification. In this work, we follow the approach developed by Boes, Egas Santander, and Kupers [5, 6], in which the compactification is built from *chord diagrams* modulo an equivalence relation. These diagrams are known as *Sullivan diagrams*.

One deep result on moduli spaces is that the gluing of surfaces defines a cobordism category. While this structure has not yet been fully translated to the setting of Sullivan diagrams, Wahl and Westerland [19] proved that this gluing operation can be modelled using Sullivan diagrams and is associative at the level of chain complexes. In this thesis we prove that this gluing is associative at the space level for Sullivan diagrams with only one outgoing boundary component.

This leads us to the central focus of the thesis: the homology of Sullivan diagrams. It is well known that the homology of moduli spaces stabilizes with respect to both boundary components and genus. This naturally raises the question of whether a similar stabilization occurs for Sullivan diagrams. In particular, we are interested in whether their homology stabilizes, and if so, determining the stable range and computing the stable homology.

This thesis answers these questions in the case of stabilization with respect to punctures and boundary components. It also lays the groundwork for future work on stabilization with respect to genus.

Classical homological stability frameworks do not work in this setup because we are looking for homological stability of spaces, not groups. A family of spaces

$$\cdots \mathcal{M}_{n-1} \to \mathcal{M}_n \to \mathcal{M}_{n+1} \cdots$$

satisfies homological stability if the induced maps in homology

$$H_i(\mathcal{M}_n; \mathbb{Z}) \to H_i(\mathcal{M}_{n+1}; \mathbb{Z})$$

are isomorphisms in a range $0 \leq i \leq f(n)$ that increase in n. This has been largely studied when $\mathcal{M}_n = BG_n$ for some group G_n. Unfortunately, it is not always possible to find such groups. So

we must use another framework for homological stability. Krannich's method [12] is designed to fit this generalisation.

The purpose of this master thesis is to fit Sullivan diagrams into Krannich's framework and get homological stability results. To do this we need to prove two things: first, the space of Sullivan diagrams forms an algebra over a Swiss-cheese-like operad; second, the connectivity of a special semi-simplicial space.

In Chapter 1 we give a quick introduction to operads. We detail the commutative operad, the little-disks operad, and different versions of the cacti operad introduced by Voronov [16]. Then we recall coloured operads and build the Swiss-cheese-like operad from Krannich [12] which plays a crucial role in his framework for homological stability.

Sullivan diagrams, the main objects of this master thesis, are defined and explored in Chapter 2. We assemble Sullivan diagrams into a topological space $\mathscr{SD}$ called the space of Sullivan diagrams. Then we study the decomposition of $\mathscr{SD}$ into pieces $\mathscr{SD}_{g,n}$ that contain Sullivan diagrams corresponding to surfaces of genus g with n incoming boundary components and 1 outgoing boundary component. After these definitions, we compute the fundamental group of spaces $\mathscr{SD}_{g,n}$ for some choices of g and n. These computations assemble into the following new result.

Theorem A (Theorem 2.3.4)**.** *The spaces $\mathscr{SD}_{g,1}$ are simply connected for all $g > 0$.*

Chapter 3 is dedicated to fit Sullivan diagrams into Krannich's framework [12] for homological stability. We start by proving that the space of Sullivan diagrams is a topological operad with the composition inherited from gluing cobordisms.

Theorem B (Corollary 3.1.4)**.** *The symmetric sequence $\{\mathscr{SD}(k)\}_{k\geq 1}$ assembles into a topological operad.*

This operadic composition is compatible with the composition of cacti operads. Specifically we prove the space of Sullivan diagrams forms an algebra over a coloured cacti operad. Then we use Hepworth's zigzag [9] to show that our coloured cacti operad is weakly equivalent to Krannich's Swiss-cheese-like operad [12]. Thus, proving the first ingredient necessary to use Krannich's results for homological stability.

The second ingredient in Krannich's framework is the connectivity of a semi-simplicial space, called *canonical resolution*. Chapter 4 is devoted to describing the canonical resolution for Sullivan diagrams. We relate it to arc complexes on surfaces which have been deeply studied for many decades. Then we use classical results by Hatcher and Wahl [8] on the connectivity of arc complexes to give the connectivity of the canonical resolution.

Homological stability results are presented in Chapter 5. Putting together all previous chapters we can apply Krannich's main theorem [12, Theorem A] to get the stable range and stable homology of Sullivan diagrams with respect to puncture/boundary stabilisation.

Theorem C (Theorem 5.1.1 and corollary 5.1.5)**.** *The stabilisation map in homology*

$$s_* : H_i(\mathscr{SD}_{g,n};\mathbb{Z}) \to H_i(\mathscr{SD}_{g,n+1};\mathbb{Z})$$

is an isomorphism for $i \leq \frac{n-1}{2}$ and an epimorphism for $i \leq \frac{n}{2}$. Furthermore, the stable homology is trivial in positive degrees.

This result also follows from [5, Theorem A] by Boes and Egas Santander. They proved that the spaces $\mathscr{SD}_{g,n}$ are $(n-2)$-connected for $g \geq 0$ and $n \geq 2$.

Additionally we present further work on the stabilisation with respect to genus. We use a coloured commutative operad to give Sullivan diagrams an algebra structure suitable for Krannich's framework [12], and discuss methods to approach the canonical resolution for genus stabilization.

Theorem D. *The space of bidecorated Sullivan diagram is a module over a commutative algebra.*

Contents

Chapter 1

Operads for homological stability

Operads were introduced by Peter May on his book [13] as a tool to study iterated loop spaces. With time, operads have proven to be very useful tools in algebraic topology and homotopy theory. This chapter starts with a brief introduction to operads with many illustrating examples. Based on this examples we describe Krannich's machinery for homological stability [12]. In further chapters we will often come back to the operads we define in this chapter.

1.1 Recollection on operads

Let $(\mathcal{E}, \oplus)$ be a symmetric monoidal category. An *operad* in $\mathcal{E}$ is a sequence $\{\mathcal{P}(k)\}_{k\in\mathbb{N}}$ of objects in $\mathcal{E}$ such that $\mathcal{P}(k)$ admits an action of the symmetric group Σ_k for all $k \in \mathbb{N}$. Intuitively think of $\mathcal{P}(k)$ as a set of k-ary operations and the symmetric group action permutes the entries. Operads are equipped with *composition maps* of the form

$$\gamma : \mathcal{P}(k) \oplus \mathcal{P}(n_1) \oplus \cdots \oplus \mathcal{P}(n_k) \to \mathcal{P}(n_1 + \cdots n_k).$$

We "plug in" the k operations of arity $n_1, \ldots, n_k$ into the operation of arity k, which yields an operation of arity $n_1 + \cdots n_k$.

Example 1.1.1. The commutative operad Com is the simplest example of an operad in the category of topological spaces. Define $Com(n) = \{*\}$ for all $n \in \mathbb{N}$, with trivial action of the symmetric groups.

Example 1.1.2. Little n-disks operad $\mathcal{D}_n$ in the monoidal category $(Top, \times)$. Let $D^n \subset \mathbb{R}^n$ be the n-dimensional open unit disk. Define

$$\mathcal{D}_n(k) = \mathrm{Emb}\left(\coprod_{1\leq i\leq k} D^n, D^n\right)$$

for all $k \geq 0$, the space of embeddings of k disjoint disks in a disk. An embedding $f \in \mathcal{D}_n(k)$ is a composition of translations and dilations only. The composition of the operad structure is

determined by

$$\gamma(f, g_1, \dots, g_k) = f \circ (g_1 \sqcup \cdots \sqcup g_k) : \coprod_{n_1+\cdots+n_k} D^n \to D^n$$

where $g_i \in \mathcal{D}_n(n_i)$ and $f \in \mathcal{D}_n(k)$.

Definition 1.1.3. An *algebra* over an operad $\mathcal{P}$ is an object $X \in \mathcal{E}$ equipped with maps

$$\theta_k : \mathcal{P}(k) \oplus X^{\oplus k} \to X$$

for all $k \geq 0$, which are associative, unital and Σ -equivariant in an appropriate sense.

Example 1.1.4. Algebras over the commutative operad Com are commutative monoids in Top. Let X be an algebra over Com. The map $Com(2) \times X^2 \to X$ defines a multiplication on X, and the map $Com(0) \to X$ defines a unit.

Example 1.1.5. An important theorem by Peter May [13] states that any n-fold loop space is an algebra over the little n-disks operad $\mathcal{D}_n$. Let Y be a pointed space, think of the n-fold loop space on Y as

$$\Omega^n(Y) = \{f : (D^n, \partial D^n) \to (Y, *)\}.$$

Then we have the maps

$$\theta_k : \mathcal{D}_n(k) \times (\Omega^n(Y))^k \to \Omega^n(Y)$$

defined by evaluating on the i-th n-fold loop on the i-th embedded disk and sending the rest of D^n to the base point.

Example 1.1.6. For any space X there are two canonical operads we can associate: the *endomorphism operad* and the *coendomorphism operad*. Define

$$End_X(k) = Map(X^k, X)$$
$$CoEnd_X(k) = Map(X, X^k)$$

where the symmetric groups act by permuting inputs and factors respectively. The composition are defined by pre-composition and post-composition respectively, both assemble into topological operads. Note that X is an algebra over End_X.

Let again $(\mathcal{E}, \oplus)$ be a symmetric monoidal category. Now assume that $\mathcal{E}$ is cocomplete and closed. We want a wider definition of operads where the inputs of operations can be distinguished by *colours*. We follow the definition by Berger and Moerdijk [3]. Let $\mathfrak{C}$ be a set (of colours), a $\mathfrak{C}$-*coloured operad* $\mathcal{P}$ is given by the data:

1. for each $n \geq 0$, and each $(n+1)$-tuple $(c_1, \cdots, c_n; c)$ of colours, an object $\mathcal{P}(c_1, \cdots, c_n; c) \in \mathcal{E}$;
2. for each colour $c \in \mathfrak{C}$, a unit $1_c : Id \to \mathcal{P}(c, c)$;
3. for each $(n+1)$-tuple $(c_1, \cdots, c_n; c)$ of colours and n other tuples of colours $\{(d_{j,1}, \dots, d_{j,k_j})\}_{j=1}^n$ a composition product

$$\gamma : \mathcal{P}(c_1, \cdots, c_n; c) \oplus \bigoplus_{j=1}^{n} \mathcal{P}(d_{j,1}, \dots, d_{j,k_j}; c_j) \to \mathcal{P}(d_{1,1}, \dots, d_{n,k_n}; c);$$

4. for each $\sigma \in \Sigma_n$, a map

$$\sigma^* : \mathcal{P}(c_1, \cdots, c_n; c) \to \mathcal{P}(c_{\sigma(1)}, \cdots, c_{\sigma(n)}; c).$$

We may think of $\mathcal{P}(c_1, \cdots, c_n; c)$ as a set of operation taking n inputs of colours $(c_1, \cdots, c_n)$ and producing an output of colour c.

Example 1.1.7. Define a coloured operad Com_2 on colours $\mathfrak{m}$ and $\mathfrak{a}$, whose space of operations $Com_2(\mathfrak{m}^l, \mathfrak{a}^k; \mathfrak{a})$ is empty for $l \neq 0$, and for $l = 1$ it is

$$Com_2(\mathfrak{a}^k; \mathfrak{a}) = \{*\}.$$

The space $Com_2(\mathfrak{m}^l, \mathfrak{a}^k; \mathfrak{m})$ is empty for $l \neq 1$, and for $l = 1$ it is

$$Com_2(\mathfrak{m}, \mathfrak{a}^k; \mathfrak{m}) = \{*\}.$$

The operadic composition in both colours is trivial. This is a coloured version of the commutative operad Com.

Example 1.1.8. Let D^2 be the 2-dimensional disk and D^2_+ be the standard unit upper semi-disk. The *Swiss cheese operad* is the two-coloured operad $\{S(m,n)\}_{m\geq 0, n\geq 1}$ where $S(m,n)$ is a subspace of embeddings

$$\mathrm{Emb}\left(\left(\coprod_m D^2\right) \coprod \left(\coprod_n D^2_+\right), D^2_+\right)$$

so that the diameter of all little semi-disks are mapped into the diameter of the big semi-disk. For more details on this example look at [15].

There are two types of composition

$$S(k,l) \times S(m_1, n_1) \times \cdots \times S(m_l, n_l) \to S(k+m, n)$$
$$S(k,l) \times S(m_1, 0) \times \cdots \times S(m_k, 0) \to S(m, l)$$

where $m = \sum_i m_i$ and $n = \sum_i n_i$. The first composition corresponds to plugging semi-disks inside semi-disks, the second composition is inherited from the little disk operad.

Example 1.1.9. Inspired from the Swiss-cheese operad, denote by $\mathcal{SC}_n$ the two-coloured operad with colours $\mathfrak{m}$ and $\mathfrak{a}$ defined as follows:

$$\mathcal{SC}_n(\mathfrak{m}^k, \mathfrak{a}^l; \mathfrak{m}) = \begin{cases} [0,\infty) \times \mathcal{D}^l(\mathbb{R}^n), & \text{if } k = 1 \\ \emptyset, & \text{otherwise} \end{cases}$$

such that if $(s, \phi) \in \mathcal{SC}_n(\mathfrak{m}, \mathfrak{a}^l; \mathfrak{m})$ then $\phi \in \mathcal{D}^l((0,s) \times (-1,1)^{n-1})$ allowing $(0, \emptyset) \in [0,\infty) \times \mathcal{D}^0(\mathbb{R}^n)$, and

$$\mathcal{SC}_n(\mathfrak{m}^k, \mathfrak{a}^l; \mathfrak{a}) = \begin{cases} \mathcal{D}^l(D^n), & \text{if } k = 0 \\ \emptyset, & \text{otherwise.} \end{cases}$$

Composition restricted to the $\mathfrak{a}$-colour is given by the composition of $\mathcal{D}^\bullet(D^n)$, while the composition

$$\gamma : \mathcal{SC}_n(\mathfrak{m}, \mathfrak{a}^l; \mathfrak{m}) \times \left(\mathcal{SC}_n(\mathfrak{m}, \mathfrak{a}^k; \mathfrak{m}) \times \left(\Pi^l_{j=1} \mathcal{SC}_n(\mathfrak{a}^{i_j}; \mathfrak{a})\right)\right) \to \mathcal{SC}_n(\mathfrak{m}, \mathfrak{a}^{k+i}; \mathfrak{m})$$

where $i = \sum_{j=1}^l i_j$, is defined by

$$\gamma\left(((s,\phi), ((s',\psi), (\varphi^1, \ldots, \varphi^l)))\right) = (s+s', (\psi, (\phi_1 \circ \varphi^1) + s', \ldots, (\phi_l \circ \varphi^l) + s')).$$

The embedding $\mathcal{D}^\bullet(D^n) \to \mathcal{D}^\bullet(D^{n+1})$ extends to an embedding of two-coloured operads

$$\mathcal{SC}_n \to \mathcal{SC}_{n+1}.$$

Definition 1.1.10. Two coloured operads are *weakly equivalent* if there is a zigzag between them that consists of morphisms of operads that are weak homotopy equivalences on all spaces of operations.

Definition 1.1.11. An $E_{1,n}$ *operad* is an operad $\mathcal{O}$ that is weakly equivalent to $\mathcal{SC}_n$. A *graded* E_1*-module* $\mathcal{M}$ *over an* E_n*-algebra* $\mathcal{A}$ is an algebra $(\mathcal{M}, \mathcal{A})$ over an $E_{1,n}$-operad $\mathcal{O}$.

Remark 1.1.12. There is a map of coloured operads $\mathcal{SC}_2 \to Com_2$, so Com_2-algebras are $E_{1,2}$-algebras.

Now we will give a brief recollection on realization systems for operads and the mapping operad. A more detail description of these notions is presented in [9, Section 2].

Definition 1.1.13. [9, Definition 2.1] Let X be a Hausdorff topological space. A *realization system* for an topological operad $\mathcal{O}$ *with boundaries* X is a rule $\mathcal{RO}$ such that for all $n \geq 0$ and any $x \in \mathcal{O}(n)$ it produces a topological $|x|$ equipped with:

- *Incoming boundary maps*
$$\partial_1, \dots, \partial_n : X \to |x|$$
and an *outgoing boundary map* $\partial_{out} : X \to |x|$;
- a *symmetry map* $\sigma^* : |x| \to |x\sigma|$ for each $\sigma \in \Sigma$;
- and given $y_i \in \mathcal{O}(m_i)$ for $i = 1, \dots, n$ a pushout
$$\begin{array}{ccc} \coprod_{i=1}^n X & \xrightarrow{\partial_{out}} & |y_1| \sqcup \cdots \sqcup |y_n| \\ {\scriptstyle \sqcup \partial_i}\downarrow & \ulcorner & \downarrow \\ |x| & \longrightarrow & |\gamma(x; y_1, \dots, y_n)| \end{array}$$
called the *pasting square*.

The realization system $\mathcal{RO}$ needs to be topologized and satisfy further conditions such as unit, symmetry, pasting boundaries and associativity. Please refer to [9, Definitions 2.2 and 2.3].

Example 1.1.14. The little n-disks operad $\mathcal{D}_n$ has a realization system with boundaries S^{n-1}. For $\varphi \in \mathcal{D}^2(n)$ define $|\varphi|$ to be the complement in D^2 of the interiors of the little disks $\mathrm{im}(\varphi_i)$ for $i = 1, \dots, n$. The incoming boundary components are the inclusions of the boundaries of the little disks. The outgoing boundary is the boundary of D^2. The symmetry map $\sigma^* : |\varphi| \to |\varphi\sigma|$ identifies both spaces as subsets of D^2. This defines adequate pasting squares. More details on the verification of axioms and conditions are in [9, Example 2.5].

Definition 1.1.15. Let $\mathcal{P}, \mathcal{Q}$ be two topological operads equipped with realizations $\mathcal{RP}, \mathcal{RQ}$ both with boundaries X. We define the *mapping operad* $\mathcal{M}$ associated to $\mathcal{P}$ and $\mathcal{Q}$. For $n \geq 0$, define the space of operations

$$\mathcal{M}(n) = \{(a, c, f) : a \in \mathcal{P}(n), c \in \mathcal{Q}(n), f \in Map(|a|, |c|), f \circ \partial_i = \partial_i, f \circ \partial_{out} = \partial_{out}\}.$$

The Σ_n-action on $\mathcal{M}(n)$ is given by

$$(a, c, f)\sigma = (a\sigma, c\sigma, \sigma^* \circ f \circ (\sigma^*)^{-1}).$$

The composition maps of $\mathcal{M}$ come from the compositions of $\mathcal{P}$ and $\mathcal{Q}$, and the pasting squares. Given $(a, c, f) \in \mathcal{M}(n)$ and $(b_i, d_i, g_i) \in \mathcal{M}(m_i)$ for $i = 1, \dots, n$ the composition is

$$\gamma\big((a, c, f); (b_1, d_1, g_1), \dots, (b_n, d_n, g_n)\big) = \big(\gamma(a; b_1, \dots, b_n), \gamma(c; d_1, \dots, d_n), \gamma(f; g_1, \dots, g_n)\big)$$

where $\gamma(f; g_1, \dots, g_n)$ is the unique map making the cube

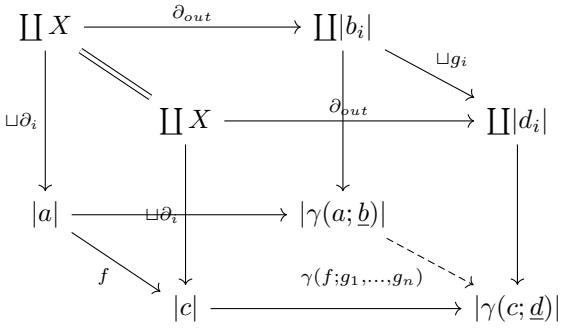

commute. We topologize $\mathcal{M}(n)$ as a subspace of the fibre-wise mapping space

$$Map_{\mathcal{P}(n)\times\mathcal{Q}(n)}(\pi_1^*\mathcal{R}\mathcal{P}(n), \pi_2^*\mathcal{R}\mathcal{Q}(n)).$$

Where π_1 and π_2 are the projections

$$\mathcal{P} \xleftarrow{\pi_1} \mathcal{M} \xrightarrow{\pi_2} \mathcal{Q}.$$

Hepworth proved that this definition assembles into a topological operad with some interesting properties

Theorem 1.1.16 ([9] Theorem 2.10)**.** *The symmetric sequence $\{\mathcal{M}(n)\}$ is a topological operad, and the projections*

$$\mathcal{P} \xleftarrow{\pi_1} \mathcal{M} \xrightarrow{\pi_2} \mathcal{Q}.$$

are morphisms of operads.

Proposition 1.1.17. *If all pasting squares of $\mathcal{R}\mathcal{P}$ and $\mathcal{R}\mathcal{Q}$ are homotopy pushouts in addition of being pushouts, then*

$$\mathcal{M}_{\simeq}(n) = \{(a, c, f) \in \mathcal{M}(n) : f \text{ is a homotopy equivalence}\}$$

forms a sub-operad $\mathcal{M}_{\simeq}$ of $\mathcal{M}$.

1.2 Different flavours of cacti operads

In the early 2000's Voronov introduced cacti in [16, Section 2.7]. Broadly speaking a *cactus* is a treelike configuration of attached parametrized circles together with a length function. In this context we refer to the circles as the *lobes* of the cactus. Each cactus comes with the data of a marked point on each lobe and a global marked point.

Later, Kaufmann defined a variant of cacti in [10, Section 2.3] where there is a global marked point, and the marked point of each lobe is the closest point to the global marked point. This variant of cacti are called *spineless cacti*. Denote by $Cact(k)$ the space of all spineless cacti on k lobes. Observe that this defines a symmetric sequence because $\mathfrak{S}_k$ acts on $Cact(k)$ by permuting the labels of the lobes.

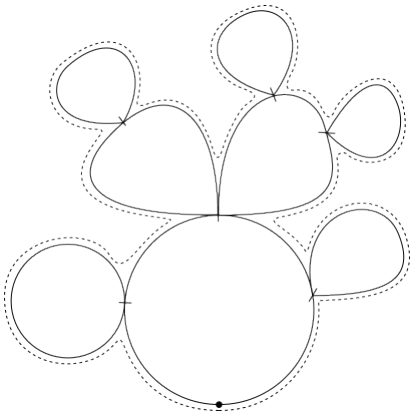

Figure 1.1: Spineless cactus on 8 lobes.

Definition 1.2.1. Let the composition of the symmetric sequence $\{Cact(k)\}_{k\geq 0}$ be given by the maps

$$\circ_i : Cact(k) \times Cact(m) \to Cact(k+m-1) \tag{1.1}$$

defined by scaling the second cactus so that its length is equal to the length of the i-th lobe of the first cactus, then identify the outside circle of the second cactus with the i-th lobe of the first cactus such that its global marked point aligns with the marked point of the i-th lobe.

This composition is associative and assembles $\{Cact(k)\}_{k\geq 0}$ into a topological operad. In [10] Kaufmann proved that $Cact$ is equivalent to the little 2-disks operad.

Theorem 1.2.2 ([10], Theorem 3.2.1)**.** *$Cact$ is an E_2-operad.*

Kaufmann defined another variant of cacti. A *spineless normalized cactus* on k lobes is a spineless cacti on k lobes where we impose the condition that all lobes have length 1. Let $Cact^1(k)$ be the space of spineless normalized cacti on k lobes.

There is a natural inclusion of spaces $Cact^1(k) \subseteq Cact(k)$, making $\{Cact^1(k)\}_{k\geq 0}$ a symmetric sequence by restricting the action. However the composition of cacti does not restrict to normalized

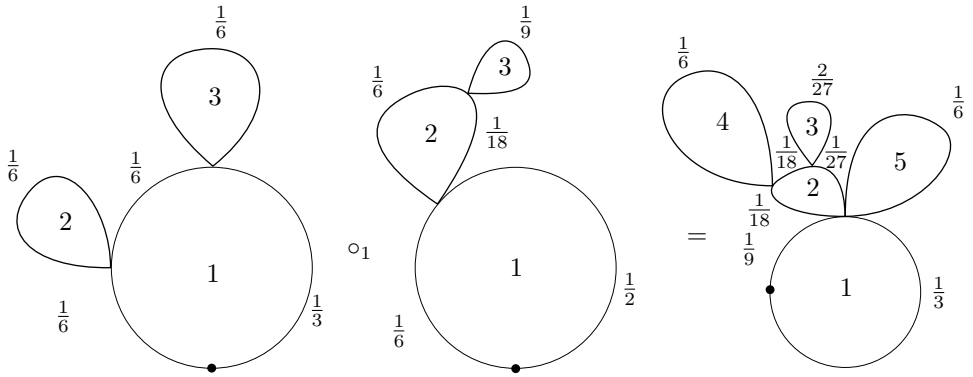

Figure 1.2: Composition of spineless cacti.

cacti. One can define a new composition by scaling the i-th lobe of the first cactus instead of the whole second cactus. It turns out that this composition is not associative, see [2, Figure 16]. So it does not assemble into an operad. Nevertheless, in [2] the authors prove that this composition is associative up to higher coherent homotopies, this means it is part of a A_∞-algebra.

Before thinking about algebras over the cacti operad, we will give a more explicit description of its spaces of operations.

Definition 1.2.3. Define $\mathcal{F}(k)$ to be the set of partitions $x = (I_1(x), \dots, I_k(x))$ of the circle $S^1 = [0,1]/0 \sim 1$ into k closed 1-manifolds, each of length $1/k$, whose interiors are pairwise disjoint, and such that there does not exist a cyclically ordered 4-tuple $(z_1; z_2; z_3; z_4) \in S^1$ with $z_1, z_3 \in \mathring{I}_j(x)$ and $z_2, z_4 \in \mathring{I}_i(x)$, for $i \neq j$.

This defines a symmetric sequence $\{\mathcal{F}(k)\}_{k\geq 1}$ where $\mathfrak{S}_k$ acts on $\mathcal{F}(k)$ by permuting the labels of the 1-manifolds.

Lemma 1.2.4 (Lemma 5.4 in [2], Section 4 in [14])**.** *The space $\mathcal{F}(k)$ is homeomorphic to $Cact^1(k)$ for all $k \geq 0$.*

Corollary 1.2.5. *There is an homeomorphism*

$$Cact(k) \cong \mathcal{F}(k) \times \mathring{\Delta}^{k-1} \tag{1.2}$$

for all $k \geq 1$.

Proof. Follows from the fact that $Cact(k) \cong Cact^1(k) \times \mathring{\Delta}^{k-1}$, see [11, Section 4.3], [10, Lemma 2.4.2] or [14, Section 4]. □

The factor in the open simplex gives the length of the lobes of the cactus. Observe that their lengths sums up to one and that there are no lobes of length zero.

Proposition 1.2.6 ([9] Proposition 4.12)**.** *There is a realization system on Cact where the incoming boundaries come from lobes, and the outgoing boundary comes from the whole boundary of the cactus.*

Example 1.2.7. Consider the cactus in Figure 1.1. In the realization, incoming boundary corresponds to lobes, and its outgoing boundary corresponds to the dashed line.

We will use the cacti operad $Cact$ and its closure $\overline{Cact}(k) = Cact^1(k) \times \Delta^{k-1}$ to define a coloured operad suitable for homological stability.

Definition 1.2.8. Define a coloured operad $\mathcal{C}$ with colours $\mathfrak{m}$ and $\mathfrak{a}$ whose space of operations $\mathcal{C}(\mathfrak{m}^l, \mathfrak{a}^k; \mathfrak{a})$ is empty for $l \neq 0$, and for $l = 1$ is

$$\mathcal{C}(\mathfrak{a}^k; \mathfrak{a}) = Cact(k).$$

The space $\mathcal{C}(\mathfrak{m}^l, \mathfrak{a}^k; \mathfrak{m})$ is empty for $l \neq 1$, and for $l = 1$ is

$$\mathcal{C}(\mathfrak{m}, \mathfrak{a}^k; \mathfrak{m}) = \overline{Cact}(k).$$

The operadic composition in colour $\mathfrak{a}$ is inherited from $Cact$. And the composition

$$\gamma : \mathcal{C}(\mathfrak{m}, \mathfrak{a}^l; \mathfrak{m}) \times \left(\mathcal{C}(\mathfrak{m}, \mathfrak{a}^k; \mathfrak{m}) \times \left(\Pi_{j=1}^l \mathcal{C}(\mathfrak{a}^{i_j}; \mathfrak{a})\right)\right) \to \mathcal{C}(\mathfrak{m}, \mathfrak{a}^{k+i}; \mathfrak{m})$$

where $i = \sum_{j=1}^l i_j$, is defined by

$$\gamma\left(C, (D, (Z_1, \ldots, Z_l))\right) = Y_0(D, C(Z_1, \ldots, Z_l)).$$

where $Y_0 \in \overline{Cact}(2)$ is the cactus with two lobes attached at the global base point, the first lobe of length 1 and the second of length0, see Figure 1.3.

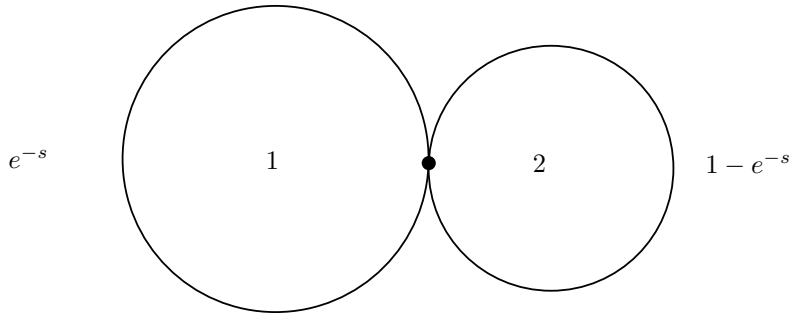

Figure 1.3: Cactus Y_s.

1.3 Homological stability

Our goal is to use operads for homological stability, more specifically we want to use Krannich's framework [12] for Sullivan diagrams. In order to do it, first we recall some important definitions from [12] mostly from Sections 1 and 2.

Let $\mathcal{M}$ be a graded E_1-module over an E_2-algebra $\mathcal{A}$ with underlying operad $\mathcal{O}$. We call a point $X \in \mathcal{A}$ *stabilizing object* if $g_{\mathcal{A}}(X) = 1$. And for an operation $c \in \mathcal{O}(\mathfrak{m}, \mathfrak{a}; \mathfrak{m})$ we call get a multiplication map $\theta(c; -, X) : \mathcal{M} \to \mathcal{M}$ that restricts to

$$\theta(c; -, X) : \mathcal{M}_n \to \mathcal{M}_{n+1}$$

for all $n \in \mathbb{N}$. From now on, fix a stabilizing object $X \in \mathcal{M}$ and an operation $c \in \mathcal{O}(\mathfrak{m}, \mathfrak{a}; \mathfrak{m})$ so that the map $\theta(c; -, X) : \mathcal{M} \to \mathcal{M}$ is also fixed. We call $s = \theta(c; -, X)$ the *stabilisation map*.

To simplify our notation we write

$$\mathcal{O}(k) = \mathcal{O}(\mathfrak{m}, \mathfrak{a}^k; \mathfrak{m})/\Sigma_k$$

and assume that the quotient $\mathcal{O}(\mathfrak{m}, \mathfrak{a}^k; \mathfrak{m}) \to \mathcal{O}(k)$ is a cover for all $k \in \mathbb{N}$. This yields composition maps

$$\gamma(-; -, 1_{\mathfrak{a}}^k) : \mathcal{O}(k) \times \mathcal{O}(l) \to \mathcal{O}(k+l).$$

Now define iterated operations $c_k \in \mathcal{O}(k)$ by setting $c_0 = 1_{\mathfrak{m}}$ and

$$c_{k+1} = \gamma(c; c_k, 1_{\mathfrak{a}}).$$

Once we have fixed an operation $c \in \mathcal{O}(\mathfrak{m}, \mathfrak{a}; \mathfrak{m})\mathcal{O}$ for our operad $\mathcal{O}$, define a topologically enriched category $U\mathcal{O} = U(\mathcal{O}, c)$ with objects $\mathbb{N}$ and morphisms

$$U\mathcal{O}([q], [p]) = \{(d, \mu) \in \mathcal{O}(p-q) \times Path_{c_{p+1}}\mathcal{O}(p+1) \,|\, \omega(\mu) = \gamma(c_{q+1}; d, 1_{\mathfrak{a}}^{q+1})\}$$

where $Path_{c_{p+1}}\mathcal{O}(p+1)$ is the space of Moore paths in $\mathcal{O}(p+1)$ starting at c_{p+1}, and $\omega(\mu)$ denotes the end-point of μ. Define composition as follows:

$$\begin{aligned} U\mathcal{O}([r], [q]) \times U\mathcal{O}([q], [p]) &\to U\mathcal{O}([r], [p]) \\ ((e, \zeta), (d, \mu)) &\mapsto (\gamma(e; d, 1_{\mathfrak{a}}^{q-l}), \mu \cdot \gamma(\zeta; d, 1_{\mathfrak{a}}^{q+1})). \end{aligned}$$

A different, but equivalent, way of defining this category is with Quillen's bracket-construction $\langle -, - \rangle$ for modules over monoidal categories.

Recall from [12, Lemma 2.7] there is a unique functor $\Delta_{inj} \to U\mathcal{B}$ where $\mathcal{B}$ is the braid category. This functor is the identity on objects, in both categories elements are given by $\mathbb{N}$. On morphisms it is fully determined by the image of the face maps $d_i \in \Delta_{inj}([p-1], [p])$, which is $b^{-1}_{X^{\oplus i} \oplus X} \oplus X^{\oplus p-1}$. It is also relevant to state [12, Lemma 2.11]: for any $E_{1,2}$-operad $\mathcal{O}$ there is an isomorphism $\pi_0 U\mathcal{O} \cong U\mathcal{B}$. Now we can proceed with our background for homological stability.

Definition 1.3.1. The *thickening of the semisimplicial category* associated to $\mathcal{O}$ is the subcategory $\tilde{\Delta}_{inj} \subseteq U\mathcal{O}$ obtained from $U\mathcal{O}$ by restricting to the path components hit by the section $\Delta_{inj} \to \pi_0 U\mathcal{O}$ coming from the functor $\Delta_{inj} \to U\mathcal{B}$ and the isomorphism $\pi_0 U\mathcal{O} \cong U\mathcal{B}$.

Definition 1.3.2. Let $\mathcal{M}$ be a graded E_1-module over an E_2-algebra $\mathcal{A}$ with underlying operad $\mathcal{O}$ with a fixed choice of stabilizing operation and object (c, X). Define the contravariant $U\mathcal{O}$-space $B_\bullet(\mathcal{M})$ by

$$B_p(\mathcal{M}) = \{(A, \zeta) \in \mathcal{M} \times Path(\mathcal{M}) \,|\, \omega(\zeta) = s^{p+1}(A)\}$$

and

$$\begin{aligned} U\mathcal{O}([q], [p]) \times B_p(\mathcal{M}) &\to B_q(\mathcal{M}) \\ ((d, \mu), (A, \zeta)) &\mapsto (\theta(d; A, X^{p-q}), \zeta \cdot \theta(\mu; A, X^{p+1})) \end{aligned}$$

The evaluation of paths at zero defines an augmentation $B_\bullet(\mathcal{M}) \to \mathcal{M}$ which is a level-wise fibration.

Definition 1.3.3. The *canonical resolution* of $\mathcal{M}$ is the fibrant augmented $\tilde{\Delta}_{inj}$-space

$$R_\bullet(\mathcal{M}) \to \mathcal{M}$$

obtained from $B_\bullet(\mathcal{M})$ by restricting to $\tilde{\Delta}_{inj} \subseteq U\mathcal{O}$.

The fibre $W_\bullet(A)$ of the canonical resolution of $\mathcal{M}$ at a point $A \in \mathcal{M}$ is a $\tilde{\Delta}_{inj}$-space called *space of destabilisations* of A.

Chapter 2

Combinatorial model of the moduli space of Riemann surfaces

An *oriented 2-cobordism* is an oriented surface S of genus g, with parametrized boundary divided into n enumerated incoming boundary components and m enumerated out-coming boundary components. We denote by $S_g^{n,m}$ the topological type of such cobordism.

Denote by $\mathrm{Diff}^+(S, \partial S)$ the *space of orientation preserving self-diffeomorphisms* of S which fix the boundary pointwise. Composition of diffeomorphism makes this space into a topological group. By the same argument, its set of connected components is also a group and we call it the *mapping class group* of S. We denote the mapping class group by

$$\mathrm{Mod}(S) = \pi_0(\mathrm{Diff}^+(S, \partial S)).$$

The classifying space of the mapping class group $S_g^{n,m}$ parametrizes all possible conformal structures on S up to equivalence. We call it the *moduli space* of $S_g^{n,m}$ and we denote it by

$$\mathcal{M}_g^{n,m} \simeq B\,\mathrm{Mod}(S).$$

Our goal is to give a combinatorial model for these moduli spaces and study it. In this chapter we introduce the so called *harmonic compactification* of the moduli space of Riemann surfaces. To do so we follow the approach of Egas-Santander [5, 6] defining some nice enough graphs so that we can relate them to our moduli spaces.

2.1 Fat graphs

Definition 2.1.1. A *combinatorial graph* is a tuple $G = (V, H, s, i)$ where V is a finite set of vertices, H is a finite set of half-edges, $s : H \to V$ is the source map, and $i : H \to H$ is an involution without fixed points. The *valence* of a vertex $v \in V$ is the number $\left|s^{-1}(v)\right|$. An *edge* is an orbit of i. Vertices of valence one are called *outer-vertices* or *leaves*. All other vertices are called *inner-vertices*.

The source map attaches half-edges to vertices, and the involution glues half-edges together. There is a geometric realization of combinatorial graphs as one should imagine. Vertices are points, and half-edges are half-intervals which are glued according to the source map and the involution.

Definition 2.1.2. A *fat graph* $\Gamma = (G, \sigma)$ is a combinatorial graph equipped with a cyclic ordering σ_v of the half edges incident at every vertex $v \in V$. This defines a permutation

$$\sigma : H \to H; h \to \sigma_{s(h)}(h)$$

such that $s\sigma = s$. We call σ the *fat structure* of Γ.

The *boundary cycles* of a fat graph $\Gamma = (G, \sigma)$ are the orbits of $\omega = \sigma \circ i$. The *boundary cycle sub-graph* of a boundary cycle $c = (h_1, \ldots, h_k)$ is the sub-graph of Γ uniquely determined by the half-edges $\{h_j, i(h_j) | h_j \neq i(h_j), 1 \leq j \leq k\}$.

Construction 2.1.3. Given a fat graph Γ we construct a *surface with decorations* S_Γ by fattening the geometric realization $|\Gamma|$. For every vertex $v \in V$ take an oriented disk D_v, and for every half-edge $h \in H$ take an oriented strip $I_h = [0, 1/2] \times [-1, 1]$. Now for every $h \in H$ glue the boundary $\{0\} \times [-1, 1]$ of the strip I_h to the disk $D_{s(h)}$ in such a way that the orientation of the strips and disks are preserved and strips are glued on disks according to the cyclic ordering σ. Then, for each edge $e = (h, \overline{h})$, we glue $\{1/2\} \times [-1, 1]$ of I_h to $\{1/2\} \times [-1, 1]$ of $I_{\overline{h}}$ with identity on the second factor. Finally, collapse to a puncture every boundary cycle which does not contain any leaf. This yields a surface with boundary such that each boundary component is attached to at least one leaf. Interpret these as marked points in the boundary.

For a fat graph Γ, the topological type of the decorated surface S_Γ is given by its genus, number of boundary components and number of punctures, plus the cyclic ordering of the marked points at the boundary.

We can think of the geometric realization $|\Gamma|$ as the spine of S_Γ. In fact there is a strong deformation retract $S_\Gamma \to |\Gamma|$. In particular these two spaces have the same Euler characteristic.

Remark 2.1.4. The number of punctures of S_Γ is the number of boundary cycles which do not contain leaves. The number of boundary components of S_Γ is the number of boundary cycles containing at least leaf. Hence the topological type of S_Γ is entirely determined by Γ.

Definition 2.1.5. A *closed fat graph* $(\Gamma, L_{in}, L_{out})$ is a fat graph Γ with ordered set of leaves L partitioned into incoming leaves L_{in} and outgoing leaves L_{out}, such that:

1. all inner-vertices have valence at least 3;
2. there is exactly one leaf on each boundary cycle, for a leaf l denote by Γ_l its corresponding boundary sub-graph.

Remark 2.1.6. Since there is exactly one leaf on each boundary cycle there are no punctures on surfaces with decorations coming from closed fat graphs.

Definition 2.1.7. A *p-admissible fat graph* Γ is closed fat graph such that the sub-graphs $\Gamma_l - l$ for all $l \in L_{out}$ are disjoint embedded circles in Γ. We call these boundary cycles $\Gamma_l - l$ *admissible*. A fat graph is *admissible* if it is p-admissible for some $p \in \mathbb{N}$.

Now we can put together these definitions into useful categories.

Definition 2.1.8. Denote by $\mathcal{Fat}$ the *category of closed fat graphs* whose objects are isomorphism classes of closed fat graphs, and morphisms $\Gamma \to \Gamma/F$ are given by collapsing to a point each tree in a forest F of Γ that does not contain any leaves. Moreover define $\mathcal{Fat}^{ad}$ the *category of admissible fat graphs* to be the full subcategory of $\mathcal{Fat}$ whose objects are isomorphism classes of admissible fat graphs.

Definition 2.1.9. A *metric p-admissible fat graph* is a pair (Γ, λ) consisting of a p-admissible fat graph Γ and a *length* function $\lambda : E_\Gamma \to [0,1]$, i.e. λ satisfies:

1. $\lambda(e) = 1$ if e is a leaf,
2. $\lambda^{-1}(0)$ is a forest in Γ and $\Gamma/\lambda^{-1}(0)$ is p-admissible,
3. for any admissible cycle C in Γ we have

$$\sum_{e \in C} \lambda(e) = 1.$$

Definition 2.1.10. Let Γ be a p-admissible fat graph, and let $n_1, \dots, n_p$ be the number of edges of each admissible cycle. For convenience denote $n = \sum_{i=1}^{p} n_i$. The *space of length functions* on Γ is defined by

$$\mathcal{M}(\Gamma) = \{\lambda : E_\Gamma \to [0,1] \,|\, \lambda \text{ is a length function}\}.$$

Give $\mathfrak{M}(\Gamma)$ the subspace topology via the natural inclusion

$$\mathcal{M}(\Gamma) \hookrightarrow \Delta^{n_1 - 1} \times \cdots \times \Delta^{n_p - 1} \times ([0,1])^{|E_\Gamma - n|}$$

Definition 2.1.11. Two metric admissible fat graphs (Γ, λ) and (Γ', λ') are *isomorphic* if there is an isomorphism of fat graphs $\varphi : \Gamma \to \Gamma'$ such that $\lambda = \lambda' \circ \varphi$.

Definition 2.1.12. Define the *space of metric admissible fat graphs* by

$$\mathcal{MFat}^{ad} = \left(\coprod_{\Gamma} \mathcal{M}(\Gamma) \right) / \sim$$

where $(\Gamma, \lambda) \sim (\Gamma', \lambda')$ if and only if $(\Gamma/\lambda^{-1}(0), \lambda) \cong (\Gamma'/\lambda'^{-1}(0), \lambda')$.

Remark 2.1.13. We can decompose $\mathcal{Fat}^{ad}$ and $\mathcal{MFat}^{ad}$ as a disjoint union by the topological type of graphs, i.e.

$$\mathcal{Fat}^{ad} = \coprod_{g,n,m} \mathcal{Fat}^{ad}_{g,n+m} \quad \& \quad \mathcal{MFat}^{ad} = \coprod_{g,n,m} \mathcal{MFat}^{ad}_{g,n+m}$$

where $\mathcal{Fat}^{ad}_{g,n+m}$ and $\mathcal{MFat}^{ad}_{g,n+m}$ are connected components corresponding to admissible fat graphs whose topological type has genus g, and $n+m$ boundary components where we marked n as incoming and m as outgoing.

2.2 Sullivan diagrams

Now we define an equivalence relation on metric p-admissible fat graphs $\sim_{SD}$, where SD stands for Sullivan diagrams. Let Γ_1, Γ_2 be two metric p-admissible fat graphs. We say that $\Gamma_1 \sim_{SD} \Gamma_2$ if they are connected by a zigzag of the following two operations:

- Sliding vertices along edges that do not belong to any admissible cycle;
- Forgetting lengths of non-admissible edges.

Definition 2.2.1. A *p-Sullivan diagram* Σ is an equivalence class of metric p-admissible fat graphs under $\sim_{SD}$. A *Sullivan diagram* Σ is a p-Sullivan diagram, for some $p \in \mathbb{N}$. The *space of Sullivan diagrams* is the quotient

$$\mathcal{SD} = \mathcal{MF}at^{ad} / \sim_{SD}$$

Note that for a Sullivan diagram Σ we can always take a representative such that we only remember the length of admissible edges.

Definition 2.2.2. The *multi-degree* of a p-Sullivan diagram Σ is the tuple $(|E_1| - 1, \dots, |E_p| - 1)$ where E_i is the set of inner-edges belonging to the i-th admissible cycle. The fat structure and admissible leaves give a canonical ordering of the inner-edges belonging to each admissible cycle. Denote by $e^i_0, \dots, e^i_{|E_i|-1}$ the inner-edges on the i-th admissible cycle. For $1 \leq i \leq p$ and $1 \leq j \leq |E_i|$ with $|E_i| > 1$, define the *faces* of Σ by

$$d^i_j(\Sigma) = \Sigma / e^i_j.$$

The length function on the face is the same except on the i-th admissible cycles where it becomes for $k \neq j$

$$\tilde{\lambda}(e^i_k) = \frac{\lambda(e^i_k)}{\sum_{\alpha \neq j} \lambda(e^i_\alpha)}.$$

Notice that the face maps $\{d^i_j\}_{i,j}$ satisfy the multi-simplicial identities. This motivates the following definition.

Definition 2.2.3. The *space of p-Sullivan diagrams* $p - \mathcal{SD}$ is the multi-semi-simplicial set with $(k_1, \dots, k_p)$-multi-simplices given by Sullivan diagrams of that multi-degree with face maps described as above.

Remark 2.2.4. Notice that the *space of Sullivan diagrams* admits a decomposition

$$\mathcal{SD} = \coprod_p p - \mathcal{SD}.$$

Remark 2.2.5. Just as for (metric) admissible fat graphs, Sullivan diagrams admit a decomposition by the topological type of the graphs:

$$p - \mathcal{SD} = \coprod_{g,m} p - \mathcal{SD}_{g,m}$$

where $p - \mathcal{SD}_{g,m}$ corresponds to Sullivan diagrams whose topological type has genus g, and $p + m$ boundary components where we marked p as outgoing and m as incoming. Here we lost the symmetry between outgoing and incoming boundary components. Notice that $m \geq 1$.

Definition 2.2.6. A boundary cycle of a Sullivan diagram is *non-degenerate* if its boundary cycle subgraph has at least one inner-edge which belongs to an admissible cycle. Otherwise we call it *degenerate*.

Remark 2.2.7. Degenerate boundary cycles can be interpreted as boundary components of length zero, so they behave as a puncture. In particular, anything we glue to such boundary has measure zero on the Sullivan diagram.

Definition 2.2.8. The *chain complex of Sullivan diagrams* $\mathcal{SD}$ is the chain complex freely generated as a $\mathbb{Z}$-module by all Sullivan diagrams. The *total degree* of a p-Sullivan diagram Σ is

$$\deg(\Sigma) = \sum_{i=1}^{p}(|E_i| - 1)$$

where E_i is the set of inner-edges belonging to the i-th admissible cycle of Σ. The *differential* of a Sullivan diagram Σ of multi-degree $(k_1, \dots, k_p)$ is

$$d(\Sigma) = \sum_{i=1}^{p}(-1)^{k_1+\cdots+k_{i-1}} \sum_{j=0}^{k_i}(-1)^j d_j^i(\Sigma).$$

Remark 2.2.9. As before we can decompose this chain complex as a direct sum indexed by the number of admissible cycles and the topological type of the diagrams:

$$\mathcal{SD} = \bigoplus_{p\geq 1} p - \mathcal{SD} \quad \& \quad p - \mathcal{SD} = \bigoplus_{S} p - \mathcal{SD}(S).$$

2.3 Fundamental group of the space of Sullivan diagrams

To prove homological stability results on the spaces of Sullivan diagrams $\mathscr{SD}_{g,m}$ it is important to understand these spaces very well. It is fair to ask what is the fundamental group of the spaces $\mathscr{SD}_{g,m}$. In [[5] Egas-Santander and Boes partially answered this question by showing $\mathscr{SD}_{g,m}$ is simply connected for $m > 2$ and $g \geq 0$.

Lemma 2.3.1 ([5] Lemma 4.12)**.** *Let $m > 2$ and $g \geq 0$. The spaces $\mathscr{SD}_{g,m}$ are simply connected.*

Now we will answer the remaining cases of this question.

Proposition 2.3.2. *The space $\mathscr{SD}_{0,1}$ is homotopic to the circle S^1.*

Proof. Taking its cellular decomposition we see that there is a unique 0-cell, a unique 1-cell, and no cell of higher dimension. Therefore $\mathscr{SD}_{0,1} \simeq S^1$. □

Corollary 2.3.3. *The fundamental group of $\mathscr{SD}_{0,1}$ is isomorphic to $\mathbb{Z}$.*

We are ready to state and prove Theorem A.

Theorem 2.3.4. *The spaces $\mathscr{SD}_{g,1}$ are simply connected for all $g > 0$.*

Proof. We take a similar approach than in [5, Lemma 4.12]. Let us study the k-skeleton of $\mathscr{SD}_{g,1}$ for $k = 0, 1, 2$. Using Seifert van Kampen this is enough to compute the fundamental group. First notice that $\mathscr{SD}_{g,1}^{(0)} = *$ because there is a single 0-cell.

To describe $\mathscr{SD}_{g,1}^{(1)}$ we classify 1-cells in three types as in [5]. We say that Σ is of type α if it has exactly two non-degenerate boundary cycles. Else, Σ exactly one non-degenerate boundary cycle. In this case, if Σ has one ghost surface then it is of type β, and if it has two ghost surfaces it is of type γ.

Back to our proof, since our diagrams have only one boundary cycle then there are no 1-cells of type α. Then we find 1 cell of type β and $2g + 1$ cells of type γ, see Figure 2.1. Let us explain

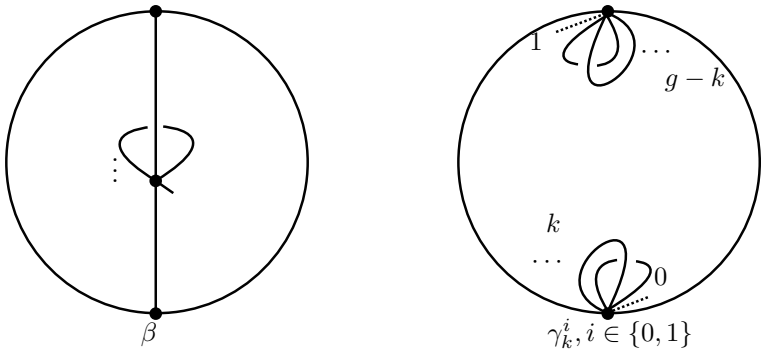

Figure 2.1: Different 1-cells in $\mathscr{SD}_{g,1}^{(1)}$.

carefully how is the cell γ_k^i defined. This is a 1-cell with exactly one non-degenerate boundary cycle and two ghost surfaces. The ghost surface attached at the vertex v_0, adjacent to the admissible leaf, has k pairs of loops that cross each other. This means that the ghost surface at this vertex has genus k. The ghost surface attached to the other vertex v_1 has $g - k$ pairs of intersecting loops, so it has genus $g - k$. The up-script $i \in \{0, 1\}$ in γ_k^i references the vertex on which the non-admissible leaf is attached to. Notice that the 1-cell γ_g^0 doesn't exist. Otherwise the vertex which doesn't have the admissible leaf would have valence (degree) 2, which is not allowed in Sullivan diagrams.

Now let us find the 2-skeleton $\mathscr{SD}_{g,1}^{(2)}$. We see that there are 2-cells of type $(\beta, \beta, \beta), (\beta, \gamma, \beta), (\gamma, \gamma, \gamma)$, see Figure 2.2.

All cells of type (β, γ, β) are of the form $(\beta, \gamma_k^i, \beta)$ for $k = 0, \ldots, g-1$ and $i \in \{0, 1\}$. There can't be a cell $(\beta, \gamma_g^i, \beta)$ because this is only possible if there are two non-degenerate boundary cycles.

There are also cells of type (γ, β, β) of the form $(\gamma_k^i, \beta, \beta)$ for $k = 1, \ldots, g - 1$ with $i \in \{0, 1\}$, and $k = g$ with $i = 1$.

Similarly we have cells of type (β, β, γ) of the form $(\beta, \beta, \gamma_k^i)$ for $k = 1, \ldots, g-1$ with $i \in \{0, 1\}$, and $k = g$ with $i = 1$.

For cells of type (γ, γ, γ) the structure depends on which vertex is the non-admissible leaf. If the non-admissible leaf is in the same vertex than the admissible leaf then the form of the 2-cell is $(\gamma_{k+l}^0, \gamma_k^0, \gamma_{g-l}^0)$ with $l > 0$ and $k + l < g$. If the non-admissible leaf isn't in the same vertex than the admissible leaf then the form of the 2-cell is $(\gamma_{k+l}^0, \gamma_k^1, \gamma_{g-l}^1)$ with $k + l < g$, or $(\gamma_{k+l}^1, \gamma_k^1, \gamma_{g-l}^0)$

with $l > 0$.

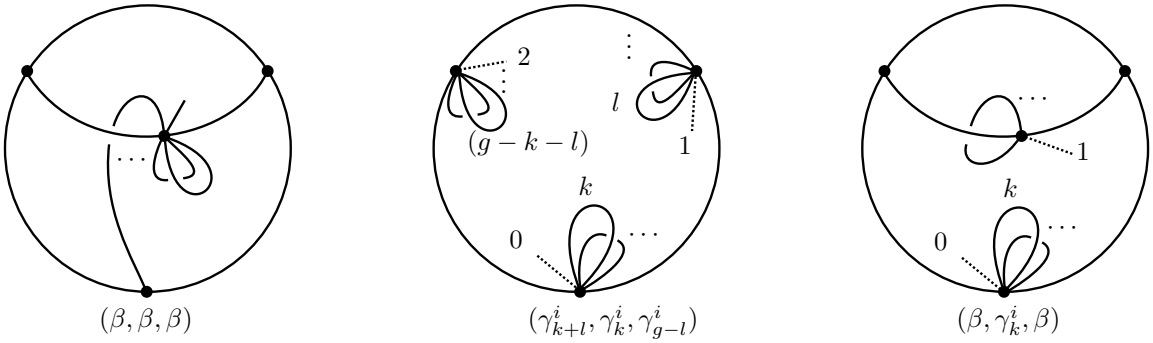

Figure 2.2: Different 2-cells in $\mathscr{SD}^{(2)}_{g,1}$.

This yields a presentation of the fundamental group of $\mathscr{SD}_{g,1}$ where 1-cell are generators and 2-cells give relations. The 2-cell of type (β, β, β) gives the relation $\beta = 1$. Together with the 2-cells of type (β, γ, β) we conclude that $\gamma^i_k = 1$ for $k = 0, \dots, g-1$ and $i \in \{0, 1\}$. It remains to see what happens with the generator corresponding to the 1-cell γ^1_g. The 2-cell of type $(\gamma^1_g, \gamma^1_0, \gamma^0_0)$ yields $\gamma^1_g = 1$.

So all generators are killed by the relations. It follows that the fundamental group is trivial. □

It remains the case $m = 2$. This turns out to be slightly more difficult and the fundamental group is non-trivial. Although it seams strange it is compatible with the calculations in the appendix of [5]. Using the cellular decomposition of the space of Sullivan diagrams we can get an intuition behind this. For $m > 2$ there are 1-cells of type α and 2-cells of type (α, α, α) and the proof of [5] relies on this. For $m = 1$ there are no 1-cells of type α but the result still holds. For $m = 2$, there are 1-cells of type α but no 2-cells of type (α, α, α) so there are no relations to kill the generators coming from 1-cells of type α.

Chapter 3

Algebra structure on the space of Sullivan diagrams

Loosely speaking, we need a pair of graded spaces $(\mathcal{M}, \mathcal{A})$ with a homotopy-commutative multiplication $\otimes : \mathcal{A} \times \mathcal{A} \to \mathcal{A}$, and a homotopy-associative action-map $\oplus : \mathcal{M} \times \mathcal{A} \to \mathcal{M}$ that satisfy various conditions, so they fit into the framework developed in [12] by Krannich. Since our goal is to prove homological stability for Sullivan diagrams we need $\mathcal{M} = \mathcal{SD}$ and $\mathcal{A}$ an E_2-algebra acting on Sullivan diagrams. For example one can take unlabelled cacti or unlabelled Sullivan diagrams as the E_2-algebra. Here the multiplication in $\mathcal{A}$ is given by composing diagrams and the module action is given by gluing along the pair of pants.

Before going into details we briefly explain the inspiration of the operations defined in this chapter. Since the space of Sullivan diagrams is the harmonic compactification of the moduli space we want to translate operations in the language of cobordisms to the language of diagrams. Let S, S' be two oriented 2-cobordisms with p respectively q outgoing boundary components, and q respectively r incoming boundary components. Since boundary components are enumerated and parametrized, we can glue the i-th outgoing boundary component of S to the i-th incoming boundary component of S', according to the parametrizations. The result is an oriented 2-cobordism, denoted $S' \circ S$, with p outgoing boundary components and r incoming boundary components. Here we define analogue operations for Sullivan diagrams.

3.1 Gluing Sullivan diagrams

How can we translate operations from the language of cobordisms to the language of Sullivan diagrams? This has been done by Wahl and Westerland [19, Section 2.8] defining an operadic composition on chain complexes. This composition has been studied by Egas-Santander [5] and Klamt [11]. We want to lift this composition to a topological version.

We focus on the case of 1-Sullivan diagrams which we denote $\mathcal{SD}$ from now on. We have a

sequence of spaces $\{\mathscr{SD}(k)\}_{k\geq 1}$ where

$$\mathscr{SD}(k) = \coprod_g \mathscr{SD}_{g,k}.$$

In other words $\mathscr{SD}(k)$ is the space of all Sullivan diagrams whose topological type has k incoming boundary components, one outgoing boundary component, and any genus. This is a symmetric sequence because $\mathfrak{S}_k$ acts on $\mathscr{SD}(k)$ by permuting the labels on the leaves corresponding to incoming boundary components.

We want to assemble this into a topological operad. To do this we define compositions

$$\circ_i : \mathscr{SD}(k) \times \mathscr{SD}(m) \to \mathscr{SD}(k+m-1).$$

Construction 3.1.1. Let $\Sigma \in \mathscr{SD}(k)$ and $\Sigma' \in \mathscr{SD}(m)$.

1. Pick fat graph representatives Γ, Γ'.
2. Cut the admissible cycle of Γ' at the admissible leaf, which yields one admissible interval to which a fat graph is attached.
3. Glue the admissible interval to the i-th incoming boundary cycle of Γ so that the endpoints of the interval coincide with the i-th incoming leaf of Γ. Then delete this leaf. Call this fat graph $\Gamma \circ_i \Gamma'$.
4. Define a metric on this fat graph scaling Σ' so that it has total length $\lambda_\Sigma(i)$. This way $\Sigma \circ_i \Sigma'$ has total length 1.

In Figure 3.1 we give an illuminating example of the composition of Sullivan diagrams.

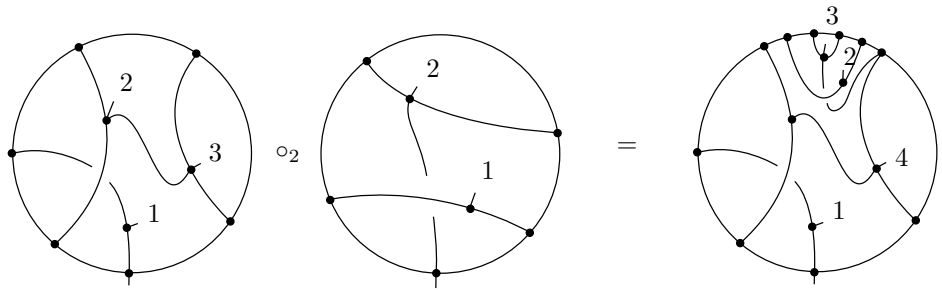

Figure 3.1: Composition of Sullivan diagrams.

Remark 3.1.2. For any two Sullivan diagrams $\Sigma \in \mathscr{SD}(k)$ and $\Sigma' \in \mathscr{SD}(m)$, the degree of their composition is at most the sum of the degrees of Σ and Σ'.

Proposition 3.1.3. *The composition of Sullivan diagrams $\circ_i$ is associative for every i.*

Proof. Let $\Sigma_i \in \mathscr{SD}(k_i)$ for $i = 1, 2, 3$. We want to prove that

$$(\Sigma_1 \circ_{\sigma_1(i)} \Sigma_2) \circ_{\sigma_2(j)} \Sigma_3 = \Sigma_1 \circ_{\sigma_1(i)} (\Sigma_2 \circ_{\sigma_2(j)} \Sigma_3). \tag{3.1}$$

By the definition of the composition of Sullivan diagrams construction 3.1.1 we know that both sides of eq. (3.1) are Sullivan diagrams whose surface with decorations have the same topological type. So to prove that they are equal we need to show that in both sides we glue the diagrams in the appropriate incoming boundary components, and that they have the same metric, i.e. the length given to all admissible edges coincide in both diagrams, see definitions 2.1.9 and 2.2.1.

In the RHS we glue Σ_3 on the j-th incoming boundary component of Σ_2 and then we glue this composed diagram on the i-th incoming boundary component of Σ_1.

In the LHS first we glue Σ_2 on the i-th incoming boundary component of Σ_1 and then we glue Σ_3 on this composition. On which boundary component are we gluing Σ_3? We glue it on the j-th component of Σ_2 which is the $(i+j-1)$-th component of $(\Sigma_1 \circ_i \Sigma_2)$. In other words

$$(\Sigma_1 \circ_{\sigma_1(i)} \Sigma_2) \circ_{\sigma_2(j)} \Sigma_3 = (\Sigma_1 \circ_{\sigma_1(i)} \Sigma_2) \circ_{(\sigma_1 \circ_i \sigma_2)(i+j-1)} \Sigma_3.$$

Therefore the Sullivan diagrams from both sides of eq. (3.1) are isomorphic as fat graphs. It remains to show that they have the same metric.

The only non-trivial part is to check it for admissible edges on the $(i+j-1)$-th boundary component of the final Sullivan diagrams.

In both sides of eq. (3.1), the admissible edges in Σ_1 that do not belong to the i-th boundary cycle keep the same length. The admissible edges in Σ_2 that do not lie on the j-th boundary component are scaled by $\lambda_3(i)$ in both sides of eq. (3.1).

Now consider the admissible edges of Σ_3. How are they scaled?

- LHS: they are scaled by $(\lambda_1 \circ_i \lambda_2)(i+j-1)$ which is equal to $\lambda_1(i)\lambda_2(j)$, the length of the j-th boundary cycle of Σ_2 after being glued (so scaled) into Σ_1.
- RHS: they are scaled twice, first by $\lambda_2(j)$ when we glue Σ_3 into Σ_2, and then by $\lambda_1(i)$ when we glue $\Sigma_2 \circ_j \Sigma_3$ into Σ_1.

In both scenarios we scale the admissible edges of Σ_3 by $\lambda_1(i)\lambda_2(j)$. Hence the metric of the Sullivan diagrams on the LHS and RHS of eq. (3.1) are the same. It follows that eq. (3.1) holds, so the composition of Sullivan diagrams is associative. □

Corollary 3.1.4 (Theorem B)**.** *The symmetric sequence $\{\mathscr{SD}(k)\}_{k\geq 1}$ assembles into a topological operad.*

Proof. We know that this is a symmetric sequence and we have proved in proposition 3.1.3 that the compositions are associative. □

One can show that, on cellular chains the translation of this operad gives the same operad presented by Wahl and Westerland [19].

3.2 Cacti and Sullivan diagrams

The previous section equip us with all necessary tools to relate cacti and Sullivan diagrams. In this section we explore the intricate relation of Sullivan diagrams and cacti.

Proposition 3.2.1. *There is a morphism of operads $Cact \to \mathscr{SD}$ such that*

$$Cact(k) \to \mathscr{SD}(k)$$

is injective and continuous for all $k \geq 1$.

Proof. Let $(x, y) \in \mathcal{F}(k) \times \mathring{\Delta}^{k-1}$ We begin by constructing a Sullivan diagram (without metric) from any partition $x \in \mathcal{F}(k)$. Then the factor $y = (y_1, \ldots, y_k) \in \mathring{\Delta}^{k-1}$ will give the metric on the admissible edges of the Sullivan diagram.

By definition any partition $x \in \mathcal{F}(k)$ can be represented in S^1. For every $1 \leq j \leq k$ consider arcs inside S^1 linking the boundary points of $I_j(x)$ following the cyclic order of S^1. The condition on $\mathcal{F}(k)$ implies that these arcs never intersect. We claim that this yields a Sullivan diagram whose topological type has k incoming boundary components, one outgoing boundary component, and genus zero.

There is one outgoing boundary component because it is a 1-Sullivan diagram. We can see that the genus is indeed zero because the arcs we draw have pairwise disjoint interiors. It remains to show that there are k incoming boundary components. Observe that each 1-manifold $I_j(x)$ together with the arcs we drew defines a region on S^1, i.e. a boundary cycle. So our claim holds.

Now we define the metric. For all $1 \leq j \leq k$ set $\lambda(I_j(x)) = y_j$, and if $I_j(k)$ is not connected then define the metric on the admissible edges preserving the proportions coming from $\mathcal{F}(k)$.

Now we prove that this map is injective. Let $(x, y), (z, w) \in \mathcal{F}(k) \times \mathring{\Delta}^{k-1}$ be two cacti which are mapped into the same Sullivan diagram Σ. Since these two cacti define the same metric it must be that $y = w$. Vertices in the admissible cycle of Σ are determined by the boundaries of the manifolds $I_j(x)$. For x and z to define the the same cell in the cellular chain complex of Sullivan diagrams it is necessary $x = z$. This finishes the proof. □

Remark 3.2.2. This maps are continuous but they are not homeomorphisms onto its images. Same goes for the restrictions $Cact(k) \to \mathscr{SD}_{0,k}$.

Intuitively one can see that cacti in $Cact(k)$ are Sullivan diagrams whose topological type is a surface of genus zero with k incoming boundary components and one outgoing boundary component, so $Cact(k) \subseteq \mathscr{SD}_{0,k}$. Moreover the composition of cacti seen as Sullivan diagrams coincides with the composition of cacti.

Corollary 3.2.3. *Any $\mathscr{SD}$-algebra is an E_2-algebra.*

Proof. Let A be an $\mathscr{SD}$-algebra. The map $Cact \to \mathscr{SD}$ from Proposition 3.2.1 induces an action of $Cact$ on A. Since $Cact$ is an E_2-operad, see Theorem 1.2.2, it follows that A is an E_2-algebra. □

Proposition 3.2.4. *$\mathscr{SD}_0$ is not an E_2-operad.*

Proof. By [5, Lemma 4.12] we know that $\mathscr{SD}_{0,k}$ is simply connected for $k > 2$. Then $\mathscr{SD}_{0,k}$ can't be weakly homotopic to $K(B_k, 1)$ for $k > 2$. This shows that $\mathscr{SD}_0$ cannot be an E_2-operad because its spaces of operations don't have the same homotopy type than the spaces of operation of the little 2-disks operad. □

Remark 3.2.5. Proposition 3.2.1 may suggest that

$$Cact(k) \cong Cact^1(k) \times \mathring{\Delta}^{k-1} \to \mathscr{SD}_{0,k}$$

is an equivalence. One may even think it is an homeomorphism, but this is not true, see Proposition 3.2.4. It might be insightful to see that $Cact^1(k) \times \Delta^{k-1} \to \mathscr{SD}_{0,k}$ is not injective. Take the metric $(1, 0, 0)$ for the two cacti in Figure 3.2. Then, both cacti are mapped to the same Sullivan diagram, represented in Figure 3.3.

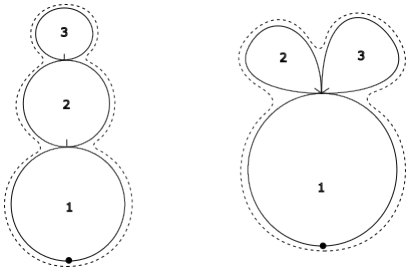

Figure 3.2: Two distinct cacti with same image in Sullivan diagrams.

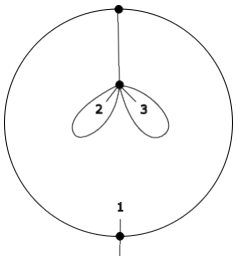

Figure 3.3: Sullivan diagram with more than one element in the preimage.

Nevertheless we can see that $\overline{Cact}(k) = Cact^1(k) \times \Delta^{k-1}$ assembles into an E_2-operad and that $\mathscr{SD}$ is also a $\overline{Cact}$-algebra.

Corollary 3.2.3 allows us to fit Sullivan diagrams into Krannich's framework [12] for homological stability with respect to boundary components or punctures. We will now use these results to show $\mathscr{SD}$ is an E_1-module over the E_2-algebra $\mathscr{SD}$, where the module comes from $Cacti$ acting on $\mathscr{SD}$ through the map in Proposition 3.2.1 and the operadic composition of Sullivan diagrams.

Recall the coloured operad $\mathcal{C}$ from Definition 1.2.8: its colours are $\mathfrak{m}$ and $\mathfrak{a}$, and its spaces of operations are

$$\mathcal{C}(\mathfrak{m}^l, \mathfrak{a}^k; \mathfrak{a}) = \begin{cases} \emptyset & l \neq 0 \\ Cact(k) & l = 0, \end{cases}$$

and

$$\mathcal{C}(\mathfrak{m}^l, \mathfrak{a}^k; \mathfrak{m}) = \begin{cases} \emptyset & l \neq 1 \\ \overline{Cact}(k) & l = 1. \end{cases}$$

Lemma 3.2.6. *Let*

$$\mathcal{A} = \coprod_k \mathcal{C}(\mathfrak{a}^k; \mathfrak{a})/\Sigma_k = \coprod_k Cact(k)/\Sigma_k.$$

Then the pair of spaces $(\mathscr{SD}, \mathcal{A})$ is an $\mathcal{C}$-algebra, where $\mathcal{C}$ is the operad from Definition 1.2.8 recalled just above.

Proof. The algebra action

$$\theta : \mathcal{C}(\mathfrak{a}^k; \mathfrak{a}) \times \mathcal{A}^k \to \mathcal{A}$$

comes from the composition of cacti. It is the action of an operad on its spaces of operations. It remains to show we have a module action. Define

$$\theta : \mathcal{C}(\mathfrak{m}, \mathfrak{a}^k; \mathfrak{m}) \times \mathscr{SD} \times \mathcal{A}^k \to \mathscr{SD}$$

by gluing cacti according to the algebra action and then glueing the Sullivan diagram and the composed cactus through the Sullivan diagram of a pair of pants of degree zero. To be more precise

$$\theta(C, \Sigma, (Z_1, \ldots, Z_k)) = L_0(\Sigma, C(Z_1, \ldots, Z_k))$$

where L_0 is the Sullivan diagram in Figure 3.4. Now we need to do the computations showing that

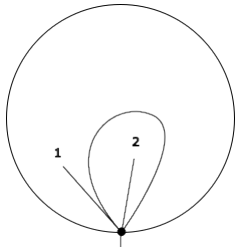

Figure 3.4: Degree zero 1-Sullivan diagram of a pair of pants.

this action is compatible with the operadic composition. Let $C \in \mathcal{C}(\mathfrak{m}, \mathfrak{a}^l; \mathfrak{m})$, $D \in \mathcal{C}(\mathfrak{m}, \mathfrak{a}^k; \mathfrak{m})$, and $(Z_1, \ldots, Z_l) \in \Pi_{j=1}^l \mathcal{C}(\mathfrak{a}^{i_j}; \mathfrak{a})$. For simplicity we will write the composition $C(Z_1, \ldots, Z_l) = C \circ Z$. Take $\Sigma \in \mathscr{SD}$, $X \in \mathcal{A}^k$ and $X' \in \mathcal{A}^i$, where $i = \sum_{j=1}^l i_j$. Then we have

$$\begin{aligned}
\theta\big(\gamma\left(C, (D, (Z_1, \ldots, Z_l))\right), \Sigma, (X', X')\big) &= \theta\big(Y_0(D, C \circ Z)\left(\Sigma, X, X'\right)\big) \\
&= L_0(\Sigma, Y_0(D, C \circ Z)(X, X')) \\
&= L_0\big(\Sigma, Y_0(D(X), C \circ Z(X'))\big) \\
&= L_0\big(L_0(\Sigma, D(X)), C \circ Z(X')\big) \\
&= \theta\big(C, \theta(D, \Sigma, X), (Z_1, \ldots, Z_l)(X')\big)
\end{aligned}$$

This finishes the proof. □

3.3 Zigzag with mapping operad

So far we have shown that Sullivan diagrams and cacti form an algebra over $\mathcal{C}$. To use this in Krannich's framework for homological stability we still need to prove $\mathcal{C}$ is an $E_{1,2}$-operad. To do so, we will give a zigzag of weak equivalences inspired from Hepworth's zigzag between little framed disks and cacti with spines [9].

Definition 3.3.1. We generalize the mapping operad construction to coloured operads. Let $\mathcal{E}$ be the coloured mapping operad associated to $\mathcal{SC}_2$ and $\mathcal{C}$. The spaces of operations on colour $\mathfrak{a}$ are

$$\mathcal{E}(\mathfrak{a}^k;\mathfrak{a}) = \{(a,c,f) : a \in \mathcal{SC}_2(\mathfrak{a}^k;\mathfrak{a}), c \in \mathcal{C}(\mathfrak{a}^k;\mathfrak{a}), f : |a| \xrightarrow{\sim} |c|, f \circ \partial = \partial\}$$

where the condition $f\circ\partial = \partial$ means that f must map the boundary of the first realization system to the boundary of the second realization system sending the marked point of each embedding to the marked point of each lobe. The spaces of operations on colour $\mathfrak{m}$ are considerably more challenging to define. We need them to be compatible with the module action of both operads $\mathcal{SC}_2$ and $\mathcal{C}$. Define

$$\mathcal{E}(\mathfrak{m},\mathfrak{a}^k;\mathfrak{m}) = \{(a,c,f,T) : a \in \mathcal{SC}_2(\mathfrak{m},\mathfrak{a}^k;\mathfrak{m}), c \in \mathcal{C}(\mathfrak{m},\mathfrak{a}^k;\mathfrak{m}), f : |a| \xrightarrow{\sim} |c|\}$$

where $T = (T_L, T_R)$ is a pair of paths from the global marked point of $|c|$ to the bottom left and right corners of $|a|$ respectively. Plus there must be a tubular neighbourhood around this paths on which f is constant equal to the global marked point of the cactus. Additionally a tuple $(a,c,f,T) \in \mathcal{E}(\mathfrak{m},\mathfrak{a}^k;\mathfrak{m})$ must satisfy that the restriction of f to $\{0,s_a\}\times[-1,1]\cup\{-1\}\times[0,s_a]$ is cst_*, where $*$ is the global marked point of the cactus, and f maps $\{-1\}\times[0,s_a]$ onto the outgoing boundary of $|c|$. By continuity we see that f must be constant equal to the marked point of the cactus below the path T.

The composition on colour $\mathfrak{a}$ comes from the mapping operad associated to $\mathcal{D}^2$ and $Cact$. Now we must define composition on colour $\mathfrak{m}$. Let us give an explicit expression for this composition. Given $(a,c,f,T) \in \mathcal{E}(\mathfrak{m},\mathfrak{a}^k;\mathfrak{m})$, $(a',c',f',T') \in \mathcal{E}(\mathfrak{m},\mathfrak{a}^l;\mathfrak{m})$ and $(b_i,d_i,g_i) \in \mathcal{E}(\mathfrak{a}_i^j;\mathfrak{a})$ for $i = 1,\dots,k$ define

$$\gamma\big((a,c,f,T);(a',c',f',T'),(b_1,d_1,g_1),\dots,(b_k,d_k,g_k)\big)$$

with the compositions of $\mathcal{SC}_2$ and $\mathcal{C}$ for the components in $\mathcal{SC}_2(\mathfrak{m},\mathfrak{a}^{k+j};\mathfrak{m})$ and $\mathcal{C}(\mathfrak{m},\mathfrak{a}^{k+j};\mathfrak{m})$, i.e.

$$\big(\gamma(a;a',b_1,\dots,b_k),\gamma(c;c',d_1,\dots,d_k),\gamma(f;f',g_1,\dots,g_k),(T_L,T'_R)\big).$$

Then define $\gamma(f;f',g_1,\dots,g_k)$ to be the unique map compatible with the boundary conditions of f and f'.

For the composition in colour $\mathfrak{m}$ it suffices to give the explicit expression for $k = j = 1$. For other values of k and j it follows from the composition in colour $\mathfrak{a}$. Take $(a,c,f,T) \in \mathcal{E}(\mathfrak{m},\mathfrak{a};\mathfrak{m})$, $(a',c',f',T') \in \mathcal{E}(\mathfrak{m},\mathfrak{a};\mathfrak{m})$ and $(b,d,g) \in \mathcal{E}(\mathfrak{a};\mathfrak{a})$. We may assume (b,d,g) is the unit. Now we will specify the weak equivalence

$$\gamma(f;f',g) : |\gamma(a;a',b)| \to |\gamma(c;c',d)|.$$

Recall that in $\mathcal{SC}_2$ we glue the rectangles on the sides $\{s_{a'}\}\times[-1,1]$ from $|a|$ and $\{0\}\times[-1,1]$ from $|a'|$. Meanwhile, in $\mathcal{C}$ we attach cacti through a wedge at the global marked point. To do the wedge

of cacti $|c| \vee |c'|$ inside the realization $|a|$ and $|a'|$ we move the global marked point of $|c'|$ through T'_L until a neighbourhood of the bottom-left corner of $|a'|$, and move the global marked point of $|c|$ through T_R until a neighbourhood of the bottom-right corner of $|a|$. Then we can glue f and f' as the desired weak equivalence $\gamma(f; f', g)$. For example, in Figures 3.5 and 3.6 we have elements in $\mathcal{E}(\mathfrak{m}, \mathfrak{a}^k; \mathfrak{m})$ where the paths T and T' are the coloured lines. Then in Figure 3.7 we see how to

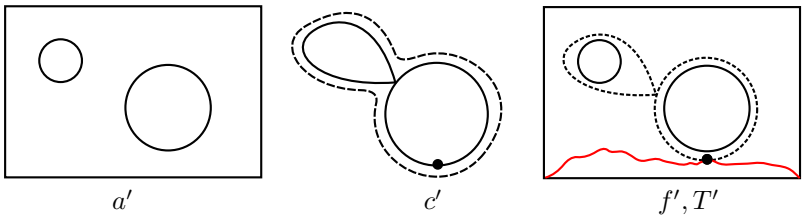

Figure 3.5: Element $(a', c', f') \in \mathcal{E}(\mathfrak{m}, \mathfrak{a}^2; \mathfrak{m})$.

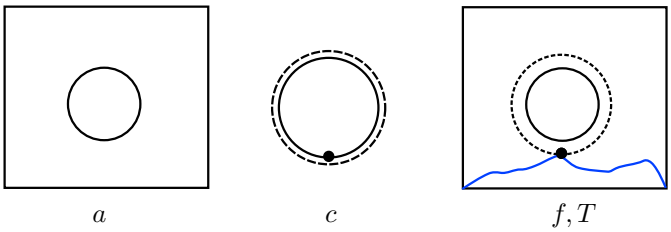

Figure 3.6: Element $(a, c, f) \in \mathcal{E}(\mathfrak{m}, \mathfrak{a}; \mathfrak{m})$.

glue the elements from Figures 3.5 and 3.6.

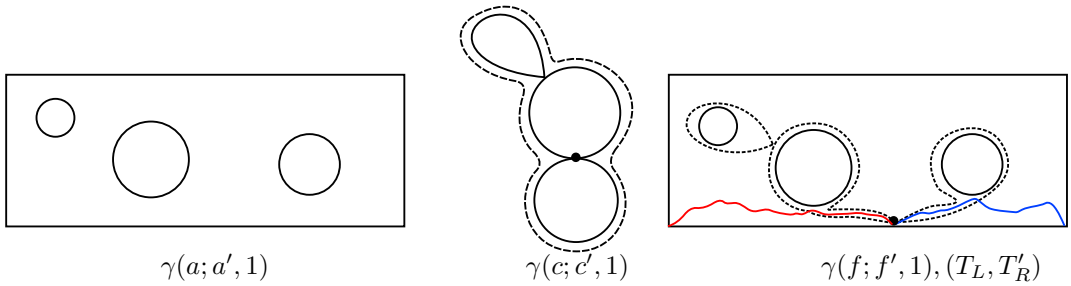

Figure 3.7: Composition in $\mathcal{E}$.

There are projection maps from our mapping operad $\mathcal{E}$ to $\mathcal{SC}_2$ and $\mathcal{C}$. Generalizing [9, Proposition 5.2] one can show that these projections $p_1 : \mathcal{E} \to \mathcal{SC}_2$ and $p_2 : \mathcal{E} \to \mathcal{SC}_2$ are morphisms of coloured operads.

To show that $\mathcal{E}$ is an $E_{1,2}$-operad we will prove that these projection maps are weak equivalences of coloured operads. For simplicity write $\mathcal{E}^{\mathfrak{c}}(k) = \mathcal{E}(\mathfrak{m}^l, \mathfrak{a}^k; \mathfrak{c})$, where $\mathfrak{c} \in \{\mathfrak{m}, \mathfrak{a}\}$. Denote by $\Pi^{\mathfrak{c}} : \mathcal{E}^{\mathfrak{c}} \to \mathcal{SC}_2^{\mathfrak{c}} \times \mathcal{C}^{\mathfrak{c}}$ the product of p_1 and p_2 on colour $\mathfrak{c}$.

Lemma 3.3.2. *The maps $p_1^{\mathfrak{a}}$ and $p_2^{\mathfrak{a}}$ are weak equivalences if and only if the maps $p_1^{\mathfrak{m}}$ and $p_2^{\mathfrak{m}}$ are weak equivalences.*

Proof. There is a commutative diagram

$$\begin{array}{ccccc} \mathcal{SC}_2^{\mathfrak{a}}(k) & \xleftarrow{p_1^{\mathfrak{a}}} & \mathcal{E}^{\mathfrak{a}}(k) & \xrightarrow{p_2^{\mathfrak{a}}} & \mathcal{C}^{\mathfrak{a}}(k) \\ \downarrow & & \downarrow & & \downarrow \\ \mathcal{SC}_2^{\mathfrak{m}}(k) & \xleftarrow[p_1^{\mathfrak{m}}]{} & \mathcal{E}^{\mathfrak{m}}(k) & \xrightarrow[p_2^{\mathfrak{m}}]{} & \mathcal{C}^{\mathfrak{m}}(k) \end{array}$$

whose vertical maps are all homotopy equivalences. The map $\mathcal{C}^{\mathfrak{a}}(k) \to \mathcal{C}^{\mathfrak{m}}(k)$ is given by the inclusion $\mathring{\Delta}^{k-1} \subseteq \Delta^{k-1}$ in

$$Cact(k) = \mathcal{F}(k) \times \mathring{\Delta}^{k-1} \hookrightarrow \mathcal{F}(k) \times \Delta^{k-1} = \overline{Cact}(k).$$

The map $\mathcal{SC}_2^{\mathfrak{a}}(k) \to \mathcal{SC}_2^{\mathfrak{a}}(k)$ is given by the inclusion of the unit disk into the rectangle of length 2, i.e.

$$\begin{array}{rcl} \mathcal{D}^2(k) & \longrightarrow & \mathcal{SC}_2^{\mathfrak{a}}(k) \\ (\varphi_1, \ldots, \varphi_k) & \longmapsto & (2, (\varphi_1 + 1, \ldots, \varphi_k + 1)) \end{array}$$

Finally, the vertical map in the middle is given by the product of the other two. Then $p_i^{\mathfrak{a}}$ is a weak equivalence if and only if $p_i^{\mathfrak{m}}$ is a weak equivalence. □

Now we will show that with $\mathcal{E}^{\mathfrak{a}}$ one can give an explicit zigzag of weak equivalences of operads between $\mathcal{D}^2$ and $Cact$. To do this it will be helpful to keep in mind the zigzag between framed disks and cacti with spines, see [9, Theorem A].

Definition 3.3.3 ([9] Definition 5.1)**.** Denote by $f\mathcal{E}$ the operad $\mathcal{M}_{\simeq}$ built from the mapping operad of framed little 2-disks $f\mathcal{D}^2$ and cacti with spines $Cacti$.

The projections $r_1 : f\mathcal{D}^2(n) \to \mathcal{D}^2(n)$ and $r_2 : Cacti(n) \to Cact(n)$ given by forgetting the framing and the spines have sections $s_1 : \mathcal{D}^2(n) \to f\mathcal{D}^2(n)$ and $s_2 : Cact(n) \to Cacti(n)$ defined by giving the canonical framing and spines.

These maps induce a projection map $r : f\mathcal{E}(n) \to \mathcal{E}^{\mathfrak{a}}(n)$ with a section $s : \mathcal{E}^{\mathfrak{a}}(n) \to f\mathcal{E}(n)$. Additionally, they are compatible with the the projections $p_1^{\mathfrak{a}}, p_2^{\mathfrak{a}}$ in the sense that the diagram

$$\begin{array}{ccccc} \mathcal{D}^2(n) & \xleftarrow{p_1^{\mathfrak{a}}} & \mathcal{E}^{\mathfrak{a}}(n) & \xrightarrow{p_2^{\mathfrak{a}}} & Cact(n) \\ \downarrow{\scriptstyle s_1} & & \downarrow{\scriptstyle s} & & \downarrow \\ f\mathcal{D}^2(n) & \longleftarrow & f\mathcal{E}(n) & \longrightarrow & Cacti(n) \\ \downarrow{\scriptstyle r_1} & & \downarrow{\scriptstyle r} & & \downarrow{\scriptstyle r_2} \\ \mathcal{D}^2(n) & \xleftarrow[p_1^{\mathfrak{a}}]{} & \mathcal{E}^{\mathfrak{a}}(n) & \xrightarrow[p_2^{\mathfrak{a}}]{} & Cact(n) \end{array}$$

commutes.

Remark 3.3.4. Notice that the inclusions $\mathcal{D}^2(n) \to f\mathcal{D}^2(n)$ and $Cact(n) \to Cacti(n)$ assemble into maps of operads $\mathcal{D}^2 \to f\mathcal{D}^2$ and $Cact \to Cacti$. However the projections $f\mathcal{D}^2(n) \to \mathcal{D}^2(n)$ and $Cacti(n) \to Cact(n)$ don't assemble into maps of operads.

Theorem 3.3.5. *The projection maps in the zigzag*

$$\mathcal{D}^2 \longleftarrow \mathcal{E}^{\mathfrak{a}} \longrightarrow Cact$$

are weak equivalences.

Proof. We will use Hepworth's results for framed disks and cacti with spines. There is a commutative diagram

$$\begin{array}{ccccc}
\mathcal{D}^2(n) & \xleftarrow{p_1^{\mathfrak{a}}} & \mathcal{E}^{\mathfrak{a}}(n) & \xrightarrow{p_2^{\mathfrak{a}}} & Cact(n) \\
\downarrow & & \downarrow & & \downarrow \\
f\mathcal{D}^2(n) & \xleftarrow{\sim} & f\mathcal{E}(n) & \xrightarrow{\sim} & Cacti(n) \\
\downarrow & & \downarrow & & \downarrow \\
\mathcal{D}^2(n) & \xleftarrow[p_1^{\mathfrak{a}}]{} & \mathcal{E}^{\mathfrak{a}}(n) & \xrightarrow[p_2^{\mathfrak{a}}]{} & Cact(n)
\end{array}$$

whose three vertical composition are the identity. By [9, Theorem A] the horizontal maps in the middle row are weak equivalences. Applying π_k to this yields the diagram

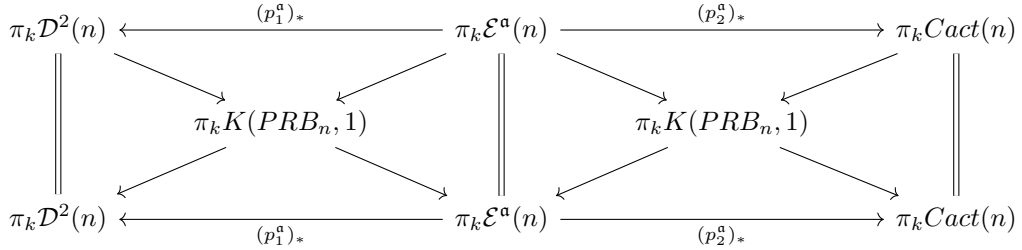

so we can deduce that $p_1^{\mathfrak{a}}, p_2^{\mathfrak{a}}$ induce isomorphisms in all homotopy groups. Recall that if a composite of two functions is injective then the first function is injective as well. Look at the upper triangles in the diagram together with this fact yield that $(p_1^{\mathfrak{a}})_*, (p_2^{\mathfrak{a}})_*$ are injective. Similarly, if a composite of two functions is surjective then the second function is surjective too. Therefore the lower triangles and this fact imply that $(p_1^{\mathfrak{a}})_*, (p_2^{\mathfrak{a}})_*$ are surjective. Hence these maps induce isomorphisms in all homotopy groups and are indeed weak homotopy equivalences. □

Corollary 3.3.6. *The operad $\mathcal{C}$ is weakly equivalent to $\mathcal{SC}_2$ through the zigzag*

$$\mathcal{SC}_2 \xleftarrow{\sim} \mathcal{E} \xrightarrow{\sim} \mathcal{C}.$$

Chapter 4

Resolution by needles

We have already discussed that the canonical resolution depends on the stabilizing object. We will focus on stability with respect to boundary components and punctures since these two cases are closely related.

Our stabilizing object X is the degree zero diagram whose decorated surface is the cylinder. Its Sullivan diagram is represented in Figure 4.1.

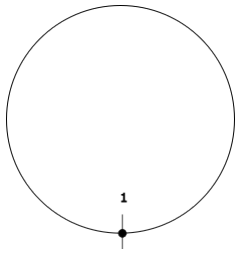

Figure 4.1: Degree zero Sullivan diagram X of the cylinder.

It remains to pick an operation $c \in \mathcal{C}(\mathfrak{m}, \mathfrak{a}; \mathfrak{m})$. Fix $c = X$. Remember that c_{k+1} is defined as $\gamma(c; c_k, 1)$. To get it we glue the cacti from c_k to X through Y_0, which is the pair of pants shown in Figure 3.4. This choice determines the sequence of operations $\{c_k\}_{k\geq 0}$. We can see that $c_k = (0, X_k)$, where $X_k \simeq \vee_k S^1$ where the first lobe has length 1 and all others have length 0.

We can finally work with the canonical resolution, introduced by Krannich in [12, Section 2]. As in Definition 1.3.3 we have an augmented $\tilde{\Delta}_{inj}$-space $R_\bullet(\mathscr{SD})$ described by

$$R_p(\mathscr{SD}) = \{(B, \zeta) \in \mathscr{SD} \times Path(\mathscr{SD}) \,|\, \omega(\zeta) = s^{p+1}(B)\}$$

and face maps

$$d_i : R_p(\mathscr{SD}) \to R_{p-1}(\mathscr{SD}); (B, \zeta) \mapsto (s(B), \zeta \cdot \theta(\mu_i; B, X^{p+1})) \tag{4.1}$$

where $\mu_i \in \Omega_{c_{p+1}}\mathcal{C}(p+1)$ is a loop corresponding to $b^{-1}_{X^{\oplus i}, X} \oplus X^{\oplus p-i}$ via the isomorphism $B_{p+1} \cong \pi_1(\mathcal{C}(p+1), c_{p+1})$. To describe this isomorphism we need the following result.

Proposition 4.0.1 (Kaufmann, Proposition 3.3.19 [10]). *The spaces $Cact(n)$ are $K(PBr_n, 1)$ spaces and the spaces $Cact(n)/S_n$ are $K(Br_n, 1)$ spaces.*

Since $(\mathcal{C}(p+1)) \cong Cact(n)/S_n$ Kaufmann's isomorphism on fundamental groups is precisely what we need to define the differential of the canonical resolution. Let σ_i be the braid on $(p+1)$ strings that twists the i-th string under the $(i+1)$-st string exactly once, see fig. 4.2. It is known

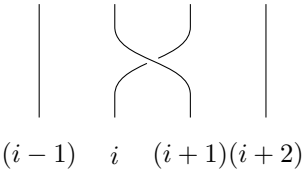

Figure 4.2: Braid generator σ_i.

that the braids $\{\sigma_i\}_i$ form a generating set of the braid group B_{p+1}, see [1, Theorem 16].

Kaufmann's isomorphism translated to Sullivan diagrams $B_{p+1} \cong \pi_1(\mathcal{C}(p+1), c_{p+1})$ sends σ_i to the path in fig. 4.3. For the original isomorphism look at [10, Figure 5]. Then μ_i corresponds

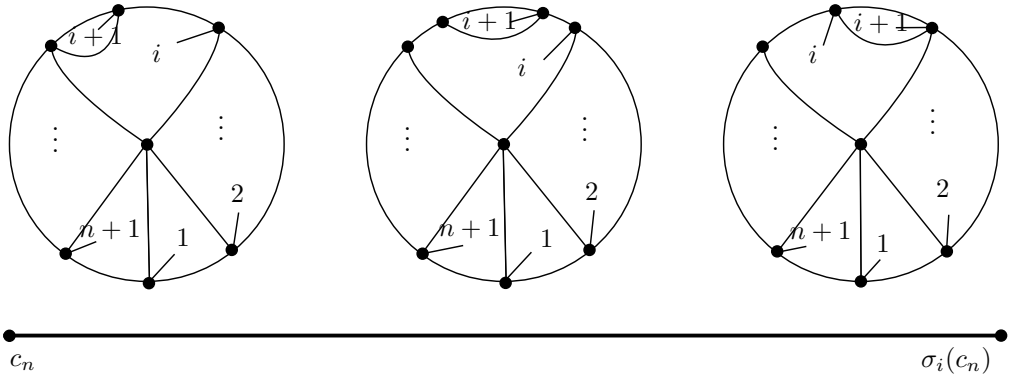

Figure 4.3: Path associated to braid generators on the Sullivan diagrams corresponding to the cactus built as a wedge of circles.

to the loop in fig. 4.4. This gives a full description of the canonical resolution. Now it remains to prove it is highly connected. By [12, Section 1.4] it is enough to compute the connectivity of the bar construction [12, Definition 1.3(i)]

$$B(U\mathcal{C}(\bullet, \blacksquare), U\mathcal{C}, B_\bullet(\mathscr{SD}))$$

because the map

$$B(U\mathcal{C}(\bullet, \blacksquare), U\mathcal{C}, B_\bullet(\mathscr{SD})) \to R_\bullet(\mathscr{SD}) \tag{4.2}$$

is a weak equivalence.

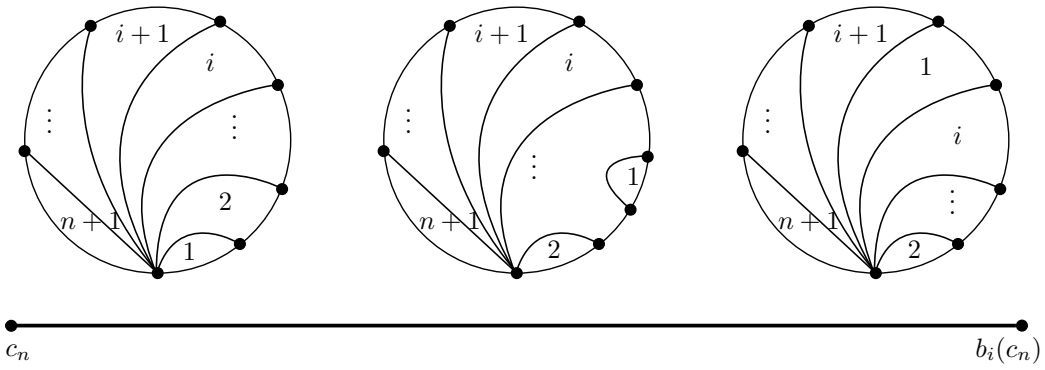

Figure 4.4: Path μ_i in Sullivan diagrams associated to $b_i = b^{-1}_{X^{\oplus i},X} \oplus X^{\oplus p-i}$

4.1 Needle complex

One can rapidly be convinced that it is difficult to prove directly that the canonical resolution is highly connected. So we define a different resolution, on which we can actually do all computations, and prove how it is related to the canonical resolution. We translate [12, Section 5] to the language of cacti and Sullivan diagrams.

The core of this section is to relate the destabilization complexes to arc complexes in Sullivan diagrams. Let $\Sigma \in \mathscr{SD}$, we are interested in isotopy classes of paths in Σ. We view $\Sigma \in Top_*$ as a pointed space, whose base-point is the vertex of the admissible leaf. Consider φ an isotopy class of paths in $Map_*(I, \Sigma)$, such that the end-point of φ is the vertex of a non-admissible leaf of Σ. Our paths must remember the label of its corresponding leaf at the end-point.

In we can map φ to an isotopy class of paths in the decorated surface S_Σ via the embedding $\Sigma \to S_\Sigma$. To define arc complexes on surfaces we often use the condition that arcs can't have any self-intersections. We want to express this condition using only the language of Sullivan diagrams.

This can be done thanks to the fat structure. Suppose φ intersects itself along a path $(v_0, \dots, v_k)$ in Σ, where (v_j, v_{j+1}) is an edge of Σ for all $j < k$. Say φ is adjacent to v_i from edges e^1_i, e^2_i for $i = 0, k$.

If the order of e^1_0, e^2_0 at v_0 is the opposite to the order of e^1_k, e^2_k at v_k coming from the fat structure of Σ, then we say that φ satisfies the *non-self-intersecting condition.*

Definition 4.1.1. An *arc* φ in a Sullivan diagram is an isotopy class of paths satisfying the non-self-intersecting condition, and remembering the label of the leaf at its endpoint, denoted by $\omega(\varphi)$.

In Sullivan diagrams Dehn twists along 0-length loops are trivial. Then we must add an equivalence relation, called *trivial twist* relation, on arcs so that this fact is taken into account. We say two arcs are equivalent, under the trivial twist relation, if they differ by any number of Dehn twists along 0-length loops. In particular this means that arcs don't care about ghost surfaces. The only thing that arcs see is a path on the admissible cycle and the non-admissible leaf they are attached to.

Definition 4.1.2. A *needle* on Σ is an equivalence class of arcs under the trivial twist relation. Denote by $\mathcal{N}(\Sigma)$ the set of needles on Σ.

A p-simplex in an arc complex on surfaces is a tuple of p arcs that don't intersect, except possible at their end-points. As before we need to write this condition in terms of the fat structure of Sullivan diagrams. It turns out it very similar to the non-self-intersecting condition.

Definition 4.1.3. Let φ, ψ be two isotopy classes of paths in a Sullivan diagram Σ. Assume that both φ and ψ pass through the path $P = (v_0, \dots, v_k)$ where each v_j is a vertex of Σ for all j, and (v_j, v_{j+1}) is an edge of Σ for all $j < k$. Denote by $e^{in}_{\varphi}, e^{out}_{\varphi}$ the edges contained in φ which are adjacent to P at v_0 and v_k respectively. Similarly denote by $e^{in}_{\psi}, e^{out}_{\psi}$ the edges for ψ. We say that φ and ψ *do not cross at* P if the cyclic ordering of $e^{in}_{\varphi}, e^{in}_{\psi}$ at v_0 is reverse to the ordering of $e^{out}_{\varphi}, e^{out}_{\psi}$ at v_k. Moreover, φ and ψ *do not cross* if they do not cross for any intersection P they have. For this we will use the notation $\varphi \parallel \psi$.

Remark 4.1.4. The notation $\varphi \parallel \psi$ is analogous to the disjoint arc condition in surfaces.

Definition 4.1.5. The *resolution by needles* is the augmented semi-simplicial space $R^{\dagger}_{\bullet}(\mathscr{SD}) \to \mathscr{SD}$ defined on p-simplices by

$$R^{\dagger}_p(\mathscr{SD}) = \coprod_{\Sigma \in \mathscr{SD}} \left\{ (\varphi_0, \dots, \varphi_p) \in \mathcal{N}(\Sigma)^{p+1} : \varphi_i \parallel \varphi_j, \omega(\varphi_i) \neq \omega(\varphi_j) \, \forall i \neq j \right\}.$$

This defines a semi-simplicial resolution of the space of Sullivan diagrams by tuples of compatible needles. In the next section, we relate this to arc complexes on surfaces.

The destabilisation complex of a Sullivan diagram Σ is the homotopy fibre of $R^{\dagger}_{\bullet}(\mathscr{SD}) \to \mathscr{SD}$ at Σ. From now on we write

$$W^{\dagger}_{\bullet}(\Sigma) = \mathrm{hofib}_{\Sigma}(R^{\dagger}_{\bullet}(\mathscr{SD}) \to \mathscr{SD}).$$

We have

$$W^{\dagger}_p(\Sigma) = \left\{ (\varphi_0, \dots, \varphi_p) \in \mathcal{N}(\Sigma)^{p+1} : \varphi_i \parallel \varphi_j, \omega(\varphi_i) \neq \omega(\varphi_j) \, \forall i \neq j \right\},$$

and call $W^{\dagger}_{\bullet}(\Sigma)$ the *non-crossing needle complex* of Σ.

We follow the approach by Hatcher and Wahl in [8]. For $\Sigma \in \mathscr{SD}$ it will be useful to consider a bigger complex. Let $E^{\dagger}_{\bullet}(\Sigma)$ be the semi-simplicial complex defined on p-simplices by

$$E^{\dagger}_p(\Sigma) = \left\{ (\varphi_0, \dots, \varphi_p) \in \mathcal{N}(\Sigma)^{p+1} : \varphi_i \parallel \varphi_j \, \forall i \neq j \right\}.$$

We call $E^{\dagger}_{\bullet}(\Sigma)$ the *needle complex* of Σ. One can see that $W^{\dagger}_{\bullet}(\Sigma) \subseteq E^{\dagger}_{\bullet}(\Sigma)$.

In terms of [8, Section 7], $E^{\dagger}_{\bullet}(\Sigma)$ is the analogue of $\mathcal{F}(S_{\Sigma}; \Delta_0, \Lambda_n)$ where Δ_0 is a singleton containing the admissible leaf, and Λ_n is the set of non-admissible leaves. Then $W^{\dagger}_{\bullet}(\Sigma)$ corresponds to $A(S_{\Sigma}; \Delta_0, \Lambda_n)$.

4.2 Zigzag of weak equivalences

Before computing the connectivity of the resolution by needles, first we show that it is equivalent to the canonical resolution. To prove this we follow Krannich's zigzag of weak equivalences in [12, Section 5]. That is, we want to demonstrate that all maps in the zigzag Equation (4.3)

$$R_\bullet(\mathscr{SD}) \leftarrow B(U\mathcal{C}(\bullet,\blacksquare), U\mathcal{C}, B_\blacksquare(\mathscr{SD})) \simeq B(U\mathcal{C}^\dagger_{\bullet,\blacksquare}, U\mathcal{C}, B_\blacksquare(\mathscr{SD})) \to R^\dagger_\bullet(\mathscr{SD}) \tag{4.3}$$

are weak equivalences. This section is dedicated to explain all the notation in this zigzag and then to show these three maps are weak equivalences. In [12, Theorem 5.5], Krannich proves that the left hand side map is a weak equivalence. It remains to adapt his proofs for the other maps in the context of cacti and Sullivan diagrams.

Let us start by defining $R^\dagger_\bullet(\mathcal{C}^\mathfrak{m})$ where $\mathcal{C}^\mathfrak{m} = \coprod_k \mathcal{C}(\mathfrak{m}, \mathfrak{a}^k; \mathfrak{a})/\Sigma_k$. For $p \geq 0$ set

$$R^\dagger_p(\mathcal{C}^\mathfrak{m}) = \coprod_{C \in \mathcal{C}^\mathfrak{m}} \left\{(\varphi_0, \dots, \varphi_p) \in \mathcal{N}(C)^{p+1} : \varphi_i \parallel \varphi_j \forall i \neq j\right\}.$$

The multiplication

$$\begin{array}{rcl} \mathcal{C}^\mathfrak{m} \times \mathcal{C}^\mathfrak{m} & \longrightarrow & \mathcal{C}^\mathfrak{m} \\ (Y, Z) & \longmapsto & \gamma(Z; Y, 1) \end{array}$$

endows $\mathcal{C}^\mathfrak{m}$ with a structure of a topological monoid. This multiplication is covered by the simplicial action

$$\Psi\colon \begin{array}{rcl} \mathcal{C}^\mathfrak{m} \times R^\dagger_\bullet(\mathcal{C}^\mathfrak{m}) & \longrightarrow & R^\dagger_\bullet(\mathcal{C}^\mathfrak{m}) \\ \big(C, (D, \varphi_0, \dots, \varphi_p)\big) & \longmapsto & \big(Y_0(C, D), Y_0(C, \varphi_0), \dots, Y_0(C, \varphi_p)\big). \end{array} \tag{4.4}$$

The cactus Y_0 is the wedge of two circles: the first of length 1 and the second of length 0. See Figure 1.3.

This action yields a $(\tilde{\Delta}^{op}_{inj} \times U\mathcal{C})$-space $U\mathcal{C}^\dagger_{\bullet,\blacksquare}$, defined on objects $([p], [k])$ as the homotopy fibre

$$U\mathcal{C}^\dagger_{p,k} = \mathrm{hofib}_{c_{k+1}}(R^\dagger_p(\mathcal{C}^\mathfrak{m}) \to \mathcal{C}^\mathfrak{m}).$$

The $\tilde{\Delta}^{op}_{inj}$-direction of $U\mathcal{C}^\dagger_{\bullet,\blacksquare}$ is induced by the semi-simplicial structure of $R^\dagger_\bullet(\mathcal{C}^\mathfrak{m})$ via the unique functor $\tilde{\Delta}_{inj} \to \Delta_{inj}$, see Definition 1.3.1. The $U\mathcal{C}$-direction is defined by

$$\begin{array}{rcl} U\mathcal{C}([k],[l]) \times U\mathcal{C}^\dagger_{\bullet,k} & \longrightarrow & U\mathcal{C}^\dagger_{\bullet,l} \\ \big((d,\mu), (e, \varphi_0, \dots, \varphi_p, \zeta)\big) & \longmapsto & \big(\Psi(d, (e, \varphi_0, \dots, \varphi_p)), \mu \cdot \gamma(\zeta; d, 1^{k+1})\big). \end{array}$$

The functoriality of this space follows from the properties of the operadic composition of $\mathcal{C}$. This space will serve as a conduct between the canonical resolution and the resolution by needles. The next lemma gives the weak equivalence in the middle of Equation (4.3).

Lemma 4.2.1. *The $(\tilde{\Delta}^{op}_{inj} \times U\mathcal{C})$-spaces $U\mathcal{C}(\bullet,\blacksquare)$ and $U\mathcal{C}^\dagger_{\bullet,\blacksquare}$ are weakly equivalent.*

Proof. Pick needles $\varphi^p = (\varphi^p_0, \dots, \varphi^p_p) \in W^\dagger_p(X^{p+1})$ such that $(c_{p+1}, \varphi^p) \in R^\dagger_p(\mathcal{C}^\mathfrak{m})$ and the order of needles $(\varphi^p_0, \dots, \varphi^p_p)$ agrees with the order of $\{\varphi^p_i\}$ induced by the fat structure of X^{p+1} at the

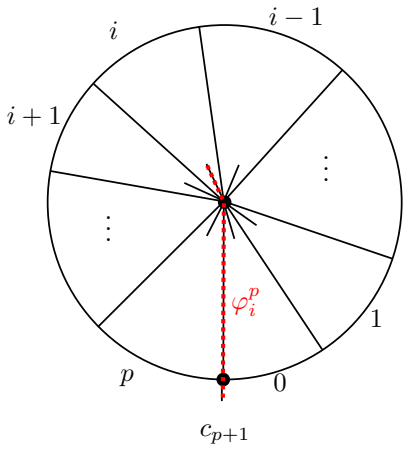

Figure 4.5: Needle φ_i^p.

admissible leaf. For example take the needles φ_i^p as in Figure 4.5. The action of $(c_{p+1}, \varphi^p, cst_{c_{p+1}})$ yields a morphism

$$U\mathcal{C}([p],[\blacksquare]) \to U\mathcal{C}^\dagger_{p,\blacksquare} \tag{4.5}$$

where

$$\begin{array}{rcl} U\mathcal{C}([p],[k]) & \longrightarrow & U\mathcal{C}^\dagger_{p,k} \\ (C,\zeta) & \longmapsto & (Y_0(C,X^{p+1}), Y_0(C,\varphi^p),\zeta). \end{array} \tag{4.6}$$

Note that this maps fits into the diagram

$$\begin{array}{ccc} U\mathcal{C}([p],[k]) & \dashrightarrow & U\mathcal{C}^\dagger_{p,k} \\ \downarrow & & \downarrow \\ \mathcal{C}^{\mathfrak{m}} & \xrightarrow{\Psi(-,(c_{p+1},\varphi^p))} & R^\dagger_p(\mathcal{C}^{\mathfrak{m}}) \\ & {\scriptstyle \gamma(c_{p+1};-,1^{p+1})} \searrow \quad \swarrow {\scriptstyle \epsilon} & \\ & \mathcal{C}^{\mathfrak{m}} & \end{array}$$

where the dotted arrow is the induced map on diagonal homotopy fibres of the commuting triangle.

There is a map $F : R^\dagger_\bullet(\mathcal{C}^{\mathfrak{m}}) \to \mathcal{C}^{\mathfrak{m}}$ that forgets all needles and leaves at the endpoints of these needles. We can see that $F \circ \Psi(-,(c_{p+1},\varphi^p)) = Id_{\mathcal{C}^{\mathfrak{m}}}$ and we get the equivalence $\Psi(-,(c_{p+1},\varphi^p)) \circ F \simeq Id_{R^\dagger_p(\mathcal{C}^{\mathfrak{m}})}$ by following leaves along needles. Therefore Equation (4.5) is an equivalence of $U\mathcal{C}$-spaces. In particular $U\mathcal{C}^\dagger_{\bullet,\blacksquare}$ is homotopy discrete. Now it remains to prove that this map is natural in $[p]$ up to homotopy. We need to show that the following square is commutative up to homotopy,

$$\begin{array}{ccc} U\mathcal{C}([p],[k]) & \longrightarrow & U\mathcal{C}^\dagger_{p,k} \\ {\scriptstyle (\tilde{d}_i)_*}\downarrow & & \downarrow{\scriptstyle (d_i)_*} \\ U\mathcal{C}([p-1],[k]) & \longrightarrow & U\mathcal{C}^\dagger_{p-1,k} \end{array}$$

where the face maps come from the choice in Figure 4.4. Let $(Z,\zeta) \in U\mathcal{C}([p],[k])$. The two compositions of the square yield the elements

$$((Y_0(Z,X^{p+1}), Y_0(Z,\varphi_0^p), \dots, \widehat{Y_0(Z,\varphi_i^p)}, \dots, Y_0(Z,\varphi_p^p)), \zeta)$$

and

$$((Y_0(Z,X^{p+1}), Y_0(Y_0(Z,X),\varphi_0^{p-1}), \dots, Y_0(Y_0(Z,X),\varphi_{p-1}^{p-1})), \zeta\cdot\gamma(\mu_i; Z, X^{p+1}))$$

The choice of needles φ_i^j ensures the existence of a path between

$$(c_{p+1}, \varphi_0^p, \dots, \widehat{\varphi_i^p}, \dots, \varphi_p^p) \text{ and } (c_{p+1}, Y_0(\varphi_0^{p-1}, X), \dots, Y_0(\varphi_{p-1}^{p-1}, X)) \tag{4.7}$$

in $R^\dagger_{p-1}(\mathcal{C}^{\mathtt{m}})$ such that it is mapped to the homotopy class of μ_i via the augmentation. Indeed, we can see that the left hand side element of Equation (4.7) has its i-th needle missing, while the right hand side element has its first needle missing. Then, going through a path in the homotopy class of μ_i, see Figure 4.4, moves the first lobe into the i-th position passing behind all other lobes. We go from the right hand side of Equation (4.7) to the left while keeping the needles unchanged. This path yields the homotopy between the two compositions of the square. □

To study the rightmost map in the zigzag, Equation (4.3), we first use the module structure to define the simplicial map

$$\begin{array}{rccc} \Phi\colon & R^\dagger_\bullet(\mathcal{C}^{\mathtt{m}}) \times \mathscr{SD} & \longrightarrow & R^\dagger_\bullet(\mathscr{SD}) \\ & \big((C,\varphi_0,\dots,\varphi_p),A\big) & \longmapsto & \big(Y_0(A,C), Y_0(A,\varphi_0),\dots,Y_0(A,\varphi_p)\big). \end{array}$$

For $k \geq 0$ we obtain simplicial maps

$$\begin{array}{rcl} U\mathcal{C}^\dagger_{\bullet,k} \times B_k(\mathscr{SD}) & \longrightarrow & R^\dagger_\bullet(\mathscr{SD})^{\mathrm{fib}} \\ \big((d,\varphi_0,\dots,\varphi_p,\mu),(A,\zeta)\big) & \longmapsto & \big(\Phi((d,\varphi_0,\dots,\varphi_p),A), \zeta\cdot\theta(\mu;A,X^{k+1})\big) \end{array} \tag{4.8}$$

Lemma 4.2.2. *The rightmost morphism in Equation* (4.3)*, i.e.*

$$B(U\mathcal{C}^\dagger_{\bullet,\blacksquare}, U\mathcal{C}, B_\blacksquare(\mathscr{SD})) \to R^\dagger_\bullet(\mathscr{SD}), \tag{4.9}$$

is a weak equivalence.

Proof. The left-hand-side and right-hand-side morphisms of Equation (4.3) fit into a commutative square.

$$\begin{array}{ccc} B(U\mathcal{C}([p],\blacksquare), U\mathcal{C}, B_\blacksquare(\mathscr{SD})) & \longrightarrow & R_p(\mathscr{SD}) \\ \simeq\downarrow & & \downarrow\simeq \\ B(U\mathcal{C}^\dagger_{p,\blacksquare}, U\mathcal{C}, B_\blacksquare(\mathscr{SD})) & \longrightarrow & R^\dagger_p(\mathscr{SD})^{\mathrm{fib}} \end{array}$$

Here the vertical morphism on the left is induced by $(c_{p+1}, \varphi^p, cst_{c_{p+1}})$ through Equation (4.5) so it is a weak equivalence. The vertical morphism on the right is induced again by $(c_{p+1}, \varphi^p, cst_{c_{p+1}})$ but this time through Equation (4.8). To show Equation (4.8) is an equivalence we use an analogous argument to the one used for Equation (4.6). Then the bottom morphism, i.e. Equation (4.9), is also a weak equivalence. □

Theorem 4.2.3. *The canonical resolution and the resolution by needles are equivalent.*

Proof. Follows from the zigzag of equivalences from Equation (4.3) together with Lemmas 4.2.1 and 4.2.2. □

4.3 Connectivity argument

Now that we have proven than the canonical resolution is weakly equivalent to the resolution by needles it is enough to determine the connectivity of the non-crossing needle complex.

Lemma 4.3.1. *There is a well defined injective simplicial morphism*

$$E^{\dagger}_{\bullet}(\Sigma) \to \mathcal{F}(S_{\Sigma}; \Delta_0, \Lambda_n)$$

which restricts to

$$W^{\dagger}_{\bullet}(\Sigma) \to A(S_{\Sigma}; \Delta_0, \Lambda_n)$$

also injective.

Proof. It suffices to see that the non-crossing property of needles is equivalent to the non-intersecting property of arcs in the decorated surface of the diagram.

Let $\Sigma \in \mathcal{SD}$ and $\varphi \in \mathcal{N}(\Sigma)$. Extend φ into a path in S_{Σ} through the inclusion $\Sigma \subset S_{\Sigma}$, i.e. $\tilde{\varphi} : I \to S_{\Sigma}$. We can see that $\tilde{\varphi}$ is a well defined arc in S_{Σ}. In fact, by construction of S_{Σ} the map

$$W^{\dagger}_0(\Sigma) \to A_0(S_{\Sigma}; \Delta_0, \Lambda_n); \varphi \mapsto \tilde{\varphi} \tag{4.10}$$

is bijective and extends to p-simplices

$$\begin{array}{rcl} W^{\dagger}_p(\Sigma) & \longrightarrow & A_p(S_{\Sigma}; \Delta_0, \Lambda_n) \\ (\varphi_0, \ldots, \varphi_p) & \longmapsto & (\tilde{\varphi}_0, \ldots, \tilde{\varphi}_p) \end{array} \tag{4.11}$$

because the non-crossing condition on needles is equivalent to the non-intersecting condition on arcs. □

Proposition 4.3.2. *Let $\Sigma \in \mathcal{SD}_{g,m}$ for some $g \geq 0$ and $m \geq 1$. The complex $E^{\dagger}_{\bullet}(\Sigma)$ is contractible, and the complex $W^{\dagger}_{\bullet}(\Sigma)$ is $(m-2)$-connected.*

Proof. These statements are true for $\mathcal{F}(S_{\Sigma}; \Delta_0, \Lambda_n)$ and $A(S_{\Sigma}; \Delta_0, \Lambda_n)$. The first was proven by Wahl [17, Lemma 2.5]. This lemma translates properly from arcs to needles because all boundary components in S_{Σ} are pure. The second was proven by Hatcher and Wahl [8, Proposition 7.2].

The trivial twist relation on Sullivan diagrams can only increase the connectivity of the needle complexes. Then the complex $E^{\dagger}_{\bullet}(\Sigma)$ is contractible, and the complex $W^{\dagger}_{\bullet}(\Sigma)$ is at least $(m-2)$-connected. □

Remark 4.3.3. It is also possible to prove this proposition by translating the techniques of Hatcher and Wahl to Sullivan diagrams. Surgery on arcs, e.g. [17, Figure 2], has an analogue for needles. The same argument of a deformation retract into a star, [18, Theorem 4.1].

Theorem 4.3.4. *The resolution by needles $R^{\dagger}_{\bullet}(\mathscr{SD})$ is graded $(g_{\mathscr{SD}}-1)$-connected.*

Proof. Remark 2.17 in [12] states that $R_\bullet(\mathcal{M})$ is graded $\phi(g_{\mathcal{M}})$-connected in degrees at least m if and only if the homotopy fibres $W_\bullet(A)$ are $(\phi(g_{\mathcal{M}}(A))-1)$-connected for all points $A \in \mathcal{M}$ with finite degree $g_{\mathcal{M}}(A) \geq m$. It is enough to check it for only one point per component of $\mathcal{M}$.

Proposition 4.3.2 together with this remark give the conclusion that $R^{\dagger}_{\bullet}(\mathscr{SD})$ is graded $(g_{\mathscr{SD}}-1)$-connected. □

Corollary 4.3.5. *The canonical resolution $R_\bullet(\mathscr{SD})$ is graded $(g_{\mathscr{SD}}-1)$-connected.*

Proof. By Theorem 4.2.3 we know that the canonical resolution is equivalent to the resolution by needles, and Theorem 4.3.4 states that the resolution by needles is $(g_{\mathscr{SD}}-1)$-connected. Then so must be the canonical resolution. □

Remark 4.3.6. It is important to mention that in the last week of the master thesis the author and supervisor realized that one should add the trivial twist condition to needles. Of course this changes many arguments but we know all results are correct because Boes and Egas Santander proved them in [5]. Adding the trivial twist condition to the destabilization complexes changed their homotopy type, but one can see that it can only increase the connectivity, so our results still hold.

Chapter 5

Results and further work

In this chapter we finally prove homological stability for Sullivan diagrams with respect to punctures and boundary components. Then we briefly discuss the stabilization with respect to genus.

5.1 Stability with respect to punctures/boundary components

The main ingredient of this section is [12, Theorem A]. To use this theorem one needs a graded E_1-module $\mathcal{M}$ over an E_2-algebra with a stabilizing object X and coefficient system. Once this setup is established, the connectivity of the canonical resolution of $\mathcal{M}$ gives the stable range in homology. In Chapter 3 we defined an $E_{1,2}$-algebra structure on the space of Sullivan diagrams $\mathcal{SD}$, and in Chapter 4 we computed the connectivity of its canonical resolution $R^{\dagger}_{\bullet}(\mathcal{SD})$. Putting all this together we get the following result.

Theorem 5.1.1. *The stabilisation map in homology*

$$s_* : H_i(\mathcal{SD}_{g,n}; \mathbb{Z}) \to H_i(\mathcal{SD}_{g,n+1}; \mathbb{Z}) \tag{5.1}$$

is an isomorphism for $i \leq \frac{n-1}{2}$ and an epimorphism for $i \leq \frac{n}{2}$.

Proof. Corollary 3.3.6 equips the space of Sullivan diagrams $\mathcal{SD}$ with a graded E_1-module structure over an E_2-algebra. The grading $g_{\mathcal{SD}} : \mathcal{SD} \to \mathbb{N}$ is given by the number of boundary components, i.e. for $\Sigma \in \mathcal{SD}_{g,n}$ we have $g_{\mathcal{SD}}(\Sigma) = n$. Let X be the Sullivan diagram in Figure 4.1, i.e. $X \simeq S^1$. This diagram X is our stabilizing object. Corollary 4.3.5 yields that the canonical resolution of $\mathcal{SD}$ is graded $\frac{g_{\mathcal{SD}}}{2}$-connected in degrees greater or equal to 1.

Then we can apply [12, Theorem A] with $g_{\mathcal{SD}}$ and $k = 2$. This gives that the stabilization map in homology

$$s_* : H_i(\mathcal{SD}_{g,n}; \mathbb{Z}) \to H_i(\mathcal{SD}_{g,n+1}; \mathbb{Z})$$

is an isomorphism for $i \leq \frac{n-1}{2}$ and an epimorphism for $i \leq \frac{n}{2}$. □

Remark 5.1.2. Boes and Egas Santander [5, Theorem A] proved a stringer statement. They show $\mathscr{SD}_{g,n}$ is $(n-2)$-connected for $g \geq 0$ and $n \geq 2$. This gives a better stable range.

Remark 5.1.3. This result agrees with the computer assisted low dimension homology computations made by Boes and Egas Santander [5, Appendix A]. They computed $H_i(\mathscr{SD}_{g,n})$ for small values of i, g, n. The homology groups computed inside the stable range from Theorem 5.1.1 are all trivial.

Now that we know that the space of Sullivan diagrams enjoys homological stability the next natural objective is to compute its stable homology. We claim that s_* is the zero map in homology and then the stable homology is zero as well.

Theorem 5.1.4. *The stabilisation map*

$$s : \mathscr{SD}_{g,m} \to \mathscr{SD}_{g,m+1}$$

induces the zero map in homology in strictly positive degrees.

Proof. The choice of stabilizing operation and object (c, X) makes sure that $s = \theta(c; -, X)$ is a cellular map. It attaches a loop at the admissible leaf, the number of vertices in the admissible cycle remains unchanged. So it maps n-cells into n-cells. Define maps

$$h_n : C_n^{cell}(\mathscr{SD}_{g,m}) \to C_{n+1}^{cell}(\mathscr{SD}_{g,m+1})$$

by attaching diagrams to a pair of pants which has both boots with positive length. We claim that this is a chain homotopy between $s_\bullet$ and the zero map. These maps fit into the following diagram.

$$\begin{array}{ccccccccc}
\cdots & \longrightarrow & C_{n+1}^{cell}(\mathscr{SD}_{g,m}) & \xrightarrow{d_{n+1}^{(m)}} & C_n^{cell}(\mathscr{SD}_{g,m}) & \xrightarrow{d_n^{(m)}} & C_{n-1}^{cell}(\mathscr{SD}_{g,m}) & \longrightarrow & \cdots \\
 & & \downarrow{\scriptstyle s_{n+1}} & \swarrow{\scriptstyle h_n} & \downarrow{\scriptstyle s_n} & \swarrow{\scriptstyle h_{n-1}} & \downarrow{\scriptstyle s_{n+1}} & & \\
\cdots & \longrightarrow & C_{n+1}^{cell}(\mathscr{SD}_{g,m+1}) & \xrightarrow[d_{n+1}^{(m+1)}]{} & C_n^{cell}(\mathscr{SD}_{g,m+1}) & \xrightarrow[d_n^{(m+1)}]{} & C_{n-1}^{cell}(\mathscr{SD}_{g,m+1}) & \longrightarrow & \cdots
\end{array}$$

To prove $s_\bullet : \widetilde{C}_\bullet^{cell}(\mathscr{SD}_{g,m}) \to \widetilde{C}_\bullet^{cell}(\mathscr{SD}_{g,m+1})$ is zero map in strictly positive degrees we must show that for $n \geq 1$

$$s_n = h_{n-1} \circ d_n^{(m)} + d_{n+1}^{(m+1)} \circ h_n. \tag{5.2}$$

For any chain $\Sigma \in C_n^{cell}(\mathscr{SD}_{g,m})$ compute

$$\begin{aligned}
(h_{n-1} \circ d_n^{(m)} + d_{n+1}^{(m+1)} \circ h_n)(\Sigma) &= \sum_{i=0}^{n} (-1)^i h_{n-1} \circ \partial_i(\Sigma) + \sum_{i=0}^{n+1} (-1)^i \partial_i \circ h_n(\Sigma) \\
&= \partial_0(h_n(\Sigma)) + \sum_{i=1}^{n+1} (-1)^i (\partial_i \circ h_n - h_{n-1} \circ \partial_{i-1})(\Sigma) \\
&= s_n(\Sigma) + \sum_{i=1}^{n+1} (-1)^i (\partial_i \circ h_n - h_{n-1} \circ \partial_{i-1})(\Sigma).
\end{aligned}$$

By definition of the differentials on the chain complex level the relation

$$\partial_i \circ h_n = h_{n-1} \circ \partial_{i-1}, \quad n, i \geq 1$$

holds because both sides collapse the $(i-1)$-st edge in the admissible cycle of Σ. Hence Equation (5.2) holds, finishing the proof. □

Corollary 5.1.5. *The stable homology of Sullivan diagrams is trivial. To be more precise,*

$$H_*(\mathscr{SD}_{g,\infty};\mathbb{Z}) = \begin{cases} \mathbb{Z} & \text{if } * = 0, \\ 0 & \text{else.} \end{cases}$$

Theorem 5.1.1 and corollary 5.1.5 prove Theorem C.

Remark 5.1.6. In [5] Egas Santander and Boes proved that $\mathscr{SD}_{g,n}$ is $(n-2)$-connected for $g \geq 0$ and $m \geq 2$.

5.2 Bidecorated fat graphs

A *bidecorated fat graph* is a fat graph with two marked leaves. This is the discrete version of bidecorated surfaces presented in [7, Section 3]. Inspired by this paper we would like to find an action of the braid groupoid on the category of bidecorated fat graphs $\mathcal{Fat}_2$.

We want monoidal structure on $\mathcal{Fat}_2$ For $\Gamma_1, \Gamma_2 \in \mathcal{Fat}_2$ define $\Gamma_1 \oplus \Gamma_2$ by attaching the leaves of Γ_1 with the leaves of Γ_2 while adding two new marked leaves. Denote by $l_j(\Gamma_i)$ the j-th leaf of Γ_i for $j \in \{0,1\}$ and $i \in \{1,2\}$. Attach $l_j(\Gamma_1)$ with $l_j(\Gamma_2)$ at a new vertex v_j. Add a new marked leaf $l_j(\Gamma_1 \oplus \Gamma_2)$ at v_j so that the cyclic ordering given by the fat structure is

$$(e_j(\Gamma_2), l_j(\Gamma_1 \oplus \Gamma_2), e_j(\Gamma_1))$$

where $e_j(\Gamma_i)$ is the edge coming from $l_j(\Gamma_i)$. This gluing can be visualized in Figure 5.1. This

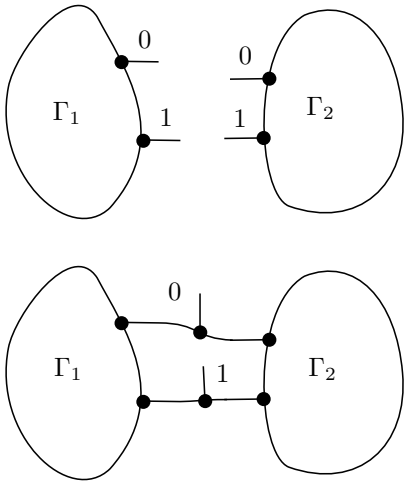

Figure 5.1: Gluing fat graphs.

yields a A_∞-monoidal category $(\mathcal{Fat}_2, \oplus, \{*\} \sqcup \{*\})$ because the monoidal product is associative up to higher homotopies. It is not strictly associative.

Example 5.2.1. Let $D \in \mathcal{Fat}_2$ be the fat graph consisting on the vertex-less edge. The graphs $(D \oplus D) \oplus D$ and $D \oplus (D \oplus D)$ are homotopic but not equal, see Figure 5.2.

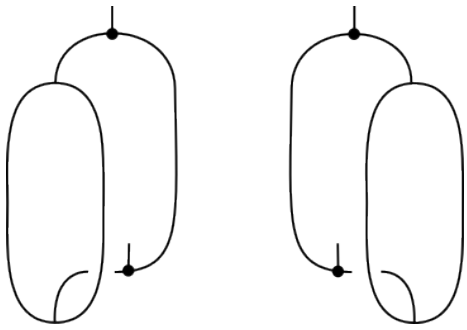

Figure 5.2: Associativity up to higher homotopies: $(D \oplus D) \oplus D$ on the left, and $D \oplus (D \oplus D)$ on the right.

So when we take π_0 we get a monoidal category $(\pi_0 \mathcal{F}at_2, \oplus, \{*\} \sqcup \{*\})$. It makes sense to consider diagrams up to homotopy because this is compatible with the equivalence relation on fat graphs to define Sullivan diagrams. A *bidecorated* Sullivan diagram is a Sullivan diagram Σ with two leaves from its set of non-admissible leaves being marked. In this case we allow incoming boundary cycles to have two leaves only when these are the two marked leaves. Denote by $\mathcal{SD}^{(2)}$ the space of bidecorated Sullivan diagrams.

Instead of defining a braiding on Sullivan diagrams it suffices to find an action of the braid groupoid. Inspired by the surface case [7], we look for the analogue of the bidecorated disk in $\mathcal{F}at_2$. Let $D \in \mathcal{F}at_2$ be the fat graph consisting on the vertex-less edge. The graphs $D, D^{\oplus 2}, D^{\oplus 3}, D^{\oplus 4}$ are represented in Figure 5.3.

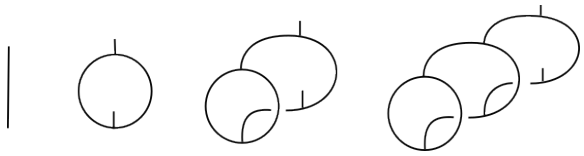

Figure 5.3: Fat graphs obtained from iteratively gluing the disks with itself.

Define a map

$$(- \oplus D) : \mathcal{SD}^{(2)} \to \mathcal{SD}^{(2)} : \Sigma \mapsto \Sigma \oplus D$$

where $\Sigma \oplus D \in \mathcal{SD}^{(2)}$ is obtained from Σ and D by identifying the marked leaves and adding two new marked leaves, one at each side of the edge we just added to the Sullivan diagram. In other words, it glues half edges to make an edge, and by doing so it adds one marked leaf at each side of the edge on the appropriate direction, see Figure 5.4. This map corresponds to the action of disk on bidecorated surfaces. Indeed, if we fatten the graphs this translates to gluing a pair of pants into one or two boundaries, exactly as the action of the bidecorated disk.

Next, we extend this map to an action of the natural numbers on the space of Sullivan diagrams

$$\theta : \mathbb{N} \times \mathcal{SD}^{(2)} \to \mathcal{SD}^{(2)}; (n, \Sigma) \mapsto \Sigma \oplus D^{\oplus n}.$$

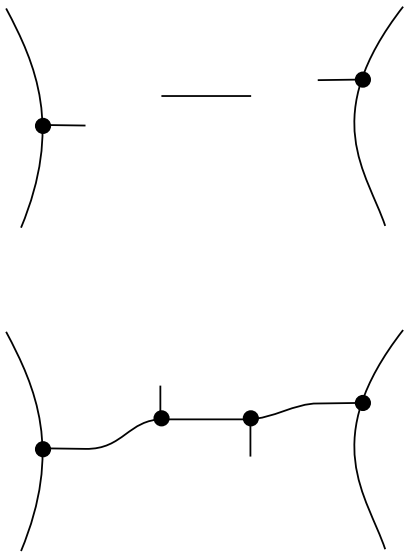

Figure 5.4: Gluing the bidecorated disk.

Recall the coloured commutative operad Com_2 from Example 1.1.7. The gluing of bidecorated disks endows Sullivan diagram with an Com_2-algebra structure, this proves Theorem D. This means that the algebra operation and the module action are strictly commutative and associative respectively, not only up to homotopy. In particular this makes the pair of spaces $(\mathscr{SD}^{(2)}, \mathbb{N})$ an $E_{1,2}$-algebra.

The remaining step is to find the appropriate destabilisation complex and compute its connectivity. Inspired by [7, Section 2] we define a disordered needle complex.

Definition 5.2.2. Let $\Sigma \in \mathscr{SD}^{(2)}$, and l_0, l_1 be the two marked leaves of Σ. Then the set of bidecorated needles in Σ, denoted by $\mathcal{N}^{\ddagger}(\Sigma)$, is the set of isotopy classes of paths $\varphi : I \to \Sigma$ such that $\varphi(0) = l_0$ and $\varphi(1) = l_1$. Furthermore, φ must satisfy the following conditions:

1. Suppose φ intersects itself along a path $(v_0, \dots, v_k)$ of Σ, where (v_j, v_{j+1}) is an edge of Σ for all $j < k$. Say φ is adjacent to v_i from edges e_i^1, e_i^2 for $i = 0, k$. The order of e_0^1, e_0^2 at v_0 must be the opposite to the order of e_k^1, e_k^2 at v_k coming from the fat structure of Σ.
2. Suppose φ is injective and that both leaves of Σ are on the same boundary component. Then φ can't follow the boundary cycle. This means that if φ is the path $e_1, \dots, e_k$ of edges in Σ then there exists $i < k$ such that the edges e_i, e_{i+1} are not adjacent to each other in the fat structure, $\sigma(e_i) \neq e_{i+1}$.

The first condition of this definition is the non-crossing condition from Definition 4.1.2, and the second condition is equivalent to the non-trivial arc condition on surfaces.

Definition 5.2.3. Let $\Sigma \in \mathscr{SD}^{(2)}$. Define its *disordered needle complex* $\mathcal{D}^{\ddagger}_{\bullet}(\Sigma)$ to be the simplicial complex whose p-simplices are determined by

$$\mathcal{D}^{\ddagger}_p(\Sigma) = \left\{(\varphi_0, \dots, \varphi_p) \in \mathcal{N}^{\ddagger}(\Sigma)^{p+1} : \varphi_i \parallel \varphi_j, \varphi_i \neq \varphi_j \, \forall i \neq j\right\},$$

and face maps forget needles.

We will use the disordered arc complex for a surface S, denoted by $\mathcal{D}^\nu(S, \Delta_0, \Delta_1)$, from [7]. Just as needles and arcs, we establish an isomorphism between disordered needles and disordered arcs.

Proposition 5.2.4. *The map of complexes*

$$\mathcal{D}^\ddagger_\bullet(\Sigma) \to \mathcal{D}^\nu(S_\Sigma, \Delta_0, \Delta_1)$$

is an isomorphism.

Proof. This proof has the same ingredients than the proof of Lemma 4.3.1 so we only give an outline of it. The non-crossing property of needles is equivalent to the non-intersecting property of arcs in the decorated surface of the diagram.

Let $\tilde{\varphi} : I \to S_\Sigma$ be the arc in S_Σ obtained by extending φ to S_Σ through $\Sigma \subset S_\Sigma$. The non-trivial needle condition on φ is equivalent to $\tilde{\varphi}$ being a non-trivial arc, in the sense that it is not isotopic to an arc in the boundary of S_Σ. This yields a map

$$\mathcal{D}^\ddagger_\bullet(\Sigma) \to \mathcal{D}^\nu(S_\Sigma, \{l_0\}, \{l_1\}); \varphi \mapsto \tilde{\varphi}.$$

As in Lemma 4.3.1 this map extends to p-simplices because of the non-crossing condition and because all elements in a tuple from $\mathcal{D}^\ddagger_p(\Sigma)$ are distinct. □

Proposition 5.2.5. *Let $\Sigma \in \mathcal{SD}^{(2)}$. The disordered needle complex $\mathcal{D}^\ddagger_\bullet(\Sigma)$ is $\left(\frac{2g+\nu-5}{3}\right)$-connected.*

Proof. Since $\mathcal{D}^\ddagger_\bullet(\Sigma)$ is isomorphic to the disordered arc complex $\mathcal{D}^\nu(S_\Sigma, \{l_0\}, \{l_1\})$ it suffices to compute the connectivity of the latter. This is done in [7, Theorem 2.4]. □

5.3 Destabilization complexes and disordered arcs

Our intuition points that the canonical resolution in the context of genus stabilisation is closely related to the disordered needle complex. Denote by $W_\bullet(\Sigma)$ the fibre of the canonical resolution over Σ, i.e. the homotopy fibre of the map $R_\bullet(\mathcal{SD}^{(2)}) \to \mathcal{SD}^{(2)}$. There is a map

$$\Phi : W_\bullet(\Sigma) \to \mathcal{D}^\ddagger_\bullet(\Sigma)$$

where $(\Gamma, \zeta) \in W_p(\Sigma)$ is mapped to the arcs $(\zeta(\varphi^p_0), \dots, \zeta(\varphi^p_p))$. Here φ^p_i denotes the arc in $D^{\oplus p+1}$ that goes around the i-th strip attached to the leafs of $D^{\oplus p+1}$. To see some examples of individual arcs φ^p_i look at Figures 5.5 to 5.8. In Figure 5.9 the tuple of arcs φ^p is represented for small values of p. Then we write $\zeta(\varphi_i)$ for the path in Σ obtained from gluing $D^{\oplus p+1}$ to Γ and following the zigzag of slides and collapses defining ζ.

Remark 5.3.1. For any $(\Gamma, \zeta) \in W_\bullet(\Sigma)$, $\Phi(\Gamma, \zeta)$ depends on the isotopy class of ζ, not on ζ itself.

This map is not injective and so far we have no reason to believe it is surjective. Nevertheless we hope it gives some insight or some tools to compute the connectivity of the destabilization complexes.

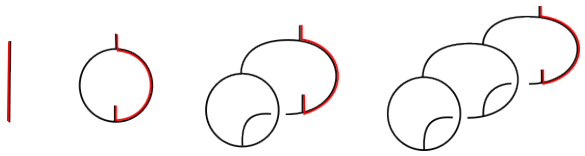

Figure 5.5: Arc φ_0^p for $p = 0, 1, 2, 3$.

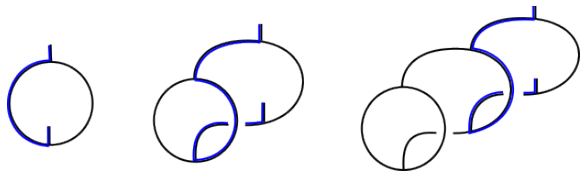

Figure 5.6: Arc φ_1^p for $p = 1, 2, 3$.

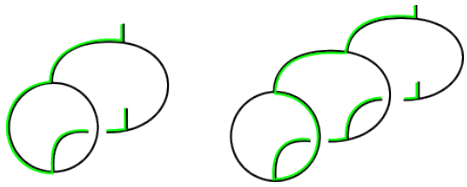

Figure 5.7: Arc φ_2^p for $p = 2, 3$.

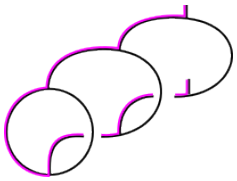

Figure 5.8: Arc φ_3^p for $p = 3, 4$.

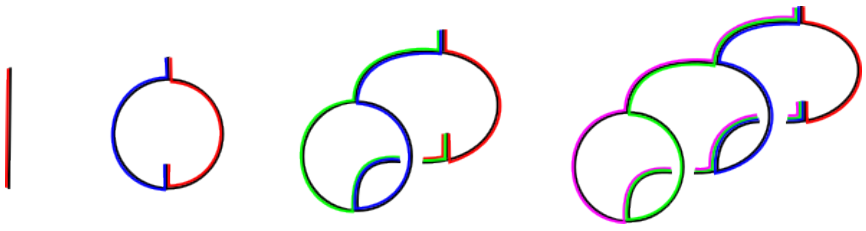

Figure 5.9: Arcs φ^p in $D^{\oplus p+1}$ for $p = 0, 1, 2, 3$.

References

[1] E. Artin. "Theory of braids". In: *Ann. of Math. (2)* 48 (1947), pp. 101–126. ISSN: 0003-486X. DOI: 10.2307/1969218. URL: https://doi.org/10.2307/1969218.

[2] Luciana Basualdo Bonatto et al. "An infinity operad of normalized cacti". In: *Topology Appl.* 316 (2022), Paper No. 108107, 54. ISSN: 0166-8641,1879-3207. DOI: 10.1016/j.topol.2022.108107. URL: https://doi.org/10.1016/j.topol.2022.108107.

[3] Clemens Berger and Ieke Moerdijk. "Resolution of coloured operads and rectification of homotopy algebras". In: *Categories in algebra, geometry and mathematical physics*. Vol. 431. Contemp. Math. Amer. Math. Soc., Providence, RI, 2007, pp. 31–58. ISBN: 978-0-8218-3970-6. DOI: 10.1090/conm/431/08265. URL: https://doi.org/10.1090/conm/431/08265.

[4] C.-F. Bödigheimer. "Configuration models for moduli spaces of Riemann surfaces with boundary". In: *Abh. Math. Sem. Univ. Hamburg* 76 (2006), pp. 191–233. ISSN: 0025-5858,1865-8784. DOI: 10.1007/BF02960865. URL: https://doi.org/10.1007/BF02960865.

[5] Felix Jonathan Boes and Daniela Egas Santander. *On the homotopy type of the space of Sullivan diagrams*. 2017. arXiv: 1705.07499 [math.AT]. URL: https://arxiv.org/abs/1705.07499.

[6] Daniela Egas Santander and Alexander Kupers. "Comparing combinatorial models of moduli space and their compactifications". In: *Algebr. Geom. Topol.* 24.2 (2024), pp. 595–654. ISSN: 1472-2747,1472-2739. DOI: 10.2140/agt.2024.24.595. URL: https://doi.org/10.2140/agt.2024.24.595.

[7] Oscar Harr, Max Vistrup, and Nathalie Wahl. "Disordered arcs and Harer stability". In: *High. Struct.* 8.1 (2024), pp. 193–223. ISSN: 2209-0606.

[8] Allen Hatcher and Nathalie Wahl. "Stabilization for mapping class groups of 3-manifolds". In: *Duke Math. J.* 155.2 (2010), pp. 205–269. ISSN: 0012-7094,1547-7398. DOI: 10.1215/00127094-2010-055. URL: https://doi.org/10.1215/00127094-2010-055.

[9] Richard Hepworth. "Groups, cacti and framed little discs". In: *Trans. Amer. Math. Soc.* 365.5 (2013), pp. 2597–2636. ISSN: 0002-9947,1088-6850. DOI: 10.1090/S0002-9947-2012-05734-5. URL: https://doi.org/10.1090/S0002-9947-2012-05734-5.

[10] Ralph M. Kaufmann. "On several varieties of cacti and their relations". In: *Algebr. Geom. Topol.* 5 (2005), pp. 237–300. ISSN: 1472-2747,1472-2739. DOI: 10.2140/agt.2005.5.237. URL: https://doi.org/10.2140/agt.2005.5.237.

[11] Angela Klamt. *Natural operations on the Hochschild complex of commutative Frobenius algebras via the complex of looped diagrams*. 2013. arXiv: 1309.4997 [math.AT]. URL: https://arxiv.org/abs/1309.4997.

[12] Manuel Krannich. "Homological stability of topological moduli spaces". In: *Geom. Topol.* 23.5 (2019), pp. 2397–2474. ISSN: 1465-3060,1364-0380. DOI: 10.2140/gt.2019.23.2397. URL: https://doi.org/10.2140/gt.2019.23.2397.

[13] J. P. May. *The geometry of iterated loop spaces*. Vol. Vol. 271. Lecture Notes in Mathematics. Springer-Verlag, Berlin-New York, 1972, pp. viii+175.

[14] Paolo Salvatore. "The topological cyclic Deligne conjecture". In: *Algebr. Geom. Topol.* 9.1 (2009), pp. 237–264. ISSN: 1472-2747,1472-2739. DOI: 10.2140/agt.2009.9.237. URL: https://doi.org/10.2140/agt.2009.9.237.

[15] Alexander A. Voronov. "The Swiss-cheese operad". In: *Homotopy invariant algebraic structures (Baltimore, MD, 1998)*. Vol. 239. Contemp. Math. Amer. Math. Soc., Providence, RI, 1999, pp. 365–373. ISBN: 0-8218-1057-X. DOI: 10.1090/conm/239/03610. URL: https://doi.org/10.1090/conm/239/03610.

[16] Alexander A. Voronov. "Notes on universal algebra". In: *Graphs and patterns in mathematics and theoretical physics*. Vol. 73. Proc. Sympos. Pure Math. Amer. Math. Soc., Providence, RI, 2005, pp. 81–103. ISBN: 0-8218-3666-8. DOI: 10.1090/pspum/073/2131012. URL: https://doi.org/10.1090/pspum/073/2131012.

[17] Nathalie Wahl. "Homological stability for the mapping class groups of non-orientable surfaces". In: *Invent. Math.* 171.2 (2008), pp. 389–424. ISSN: 0020-9910,1432-1297. DOI: 10.1007/s00222-007-0085-7. URL: https://doi.org/10.1007/s00222-007-0085-7.

[18] Nathalie Wahl. "Homological stability for mapping class groups of surfaces". In: *Handbook of moduli. Vol. III*. Vol. 26. Adv. Lect. Math. (ALM). Int. Press, Somerville, MA, 2013, pp. 547–583. ISBN: 978-1-57146-259-6.

[19] Nathalie Wahl and Craig Westerland. "Hochschild homology of structured algebras". In: *Adv. Math.* 288 (2016), pp. 240–307. ISSN: 0001-8708,1090-2082. DOI: 10.1016/j.aim.2015.10.017. URL: https://doi.org/10.1016/j.aim.2015.10.017.